Journal of Sedimentary Research

Journal of Sedimentary Research, 2005, v. 75, 663–679
DOI: 10.2110/jsr.2005.055

1926 SEPM Society for Sedimentary Geology

EARLIEST TRIASSIC CLAYSTONE BRECCIAS AND SOIL-EROSION CRISIS

G.J. RETALLACK
Department of Geological Sciences, University of Oregon, Eugene, Oregon 97403-1272, U.S.A.

ABSTRACT: **Chemostratigraphic methods ($\delta^{13}C_{org}$) for pinpointing the Permian–Triassic boundary in nonmarine rocks of Antarctica, Australia, and South Africa have drawn attention to unusual claystone breccias at this horizon of the greatest extinction in the history of life on Earth. These rocks differ from other breccias in having a high proportion of clasts with birefringence microfabrics (sepic plasmic fabrics) characteristic of soils, and can be called sepic pedoliths in the terminology of soil science. At many localities, earliest Triassic sepic pedoliths are thin (5–15 cm) beds, but some fill shallow paleochannels, and pinch out laterally. Other non-marine breccias at the Permian–Triassic boundary are dominated by fragments of coal, pedogenic carbonate nodules, and deeply weathered volcanic rock fragments. Earliest Triassic sepic pedoliths record an unusually severe and widespread episode of soil erosion associated with forest dieback at the Permian–Triassic boundary. Comparable sepic pedoliths are found in debris flows after clear-cutting of forests in western Oregon today. Studies of these modern deposits show that sepic soil peds do not withstand weathering for more than a few months. Such clayey clasts are held together mainly by roots and fungi, which decay rapidly in soils and streams. These modern analogs demonstrate that terminal Permian soil erosion was rapid and profound. Sepic pedoliths are also known at other times of mass extinction, such as the Triassic–Jurassic boundary, but are not yet known before the Devonian advent of trees and forested clayey soils.**

INTRODUCTION

The Permian–Triassic mass extinction 251 million years ago was not only the greatest mass extinction in the history of life (Jin et al. 2000), but a massive disruption of sedimentary systems, including the long-term destruction of peat-forming swamps (Retallack et al. 1996) and coral reefs (Flügel 1994), and spread of braided streams (Ward et al. 2000), anomalous sea-floor calcite (Knoll et al. 1996), calcimicrobial mounds (Lehrmann et al. 2003), and stromatolites (Schubert and Bottjer 1992). In addition there are anomalous and distinctive horizons of claystone breccia (Retallack 1999a; Retallack and Krull 1999), and flat-pebble conglomerate (Wignall and Twitchett 1999). Claystone breccias have granule-size or larger clasts that are angular, far from spherical, and have no internal bedding, unlike flat-pebble conglomerates which contain rounded and internally bedded slabs. Although Pettijohn (1975) argued that the term breccia should be restricted to rocks fragmented by faulting, volcanic intrusion, and hydrothermal pressure, breccia has been widely used for coarse-grained sharpstone sedimentary rocks (Laznicka 1988). These sedimentary breccias contain abundant clayey clasts which show signs of prior pedogenic modification (sepic plasmic fabric, sesquans, argillans, and crystallaria of Brewer 1976), suggesting that they are products of soil erosion (Retallack 1999a; Retallack and Krull 1999; Retallack et al. 2003) following terminal Permian dieback of vegetation (Retallack 1995; Twitchett et al. 2001; Looy et al. 2001). Discovery of faint iridium anomalies (Retallack et al. 1998), fullerenes with extraterrestrial ^{3}He (Poreda and Becker 2003), and carbonaceous chondritic meteoritic debris (Basu et al. 2003) within and near earliest Triassic claystone breccias opens the possibility that they might be ejecta from asteroid or comet impact. Earliest Triassic claystone breccias also include bipyramidal quartz and volcanic rock fragments (Retallack et al. 1998) from nearby volcanic arcs, opening the possibility that they are volcanic breccias. These and other plausible origins of these enigmatic rocks will be examined here, along with comparable modern deposits formed in the aftermath of forest clear-cutting in the Coast Range and Cascade Mountains of Oregon.

DESCRIPTIONS OF PERMIAN–TRIASSIC BOUNDARY BRECCIAS

The Permian–Triassic boundary is defined within global stratotype marine strata near Meishan in China by the first appearance of the conodont *Hindeodus parvus,* which is also very close in time to a marked negative anomaly in the isotopic composition of carbonate carbon (Jin et al. 2000). This carbon isotope anomaly in carbonate and organic matter has now been used to pinpoint the Permian–Triassic boundary in marine and nonmarine rocks worldwide (Morante 1996; Wignall et al. 1998; Krull and Retallack 2000; MacLeod et al. 2000; de Wit et al. 2002). This newly applied chemostratigraphic marker has been found to coincide with unusual claystone breccias at many locations (Fig. 1). Breccia beds at the boundary between latest Permian and Triassic fluvial strata are described here from Graphite Peak and Mt Crean in Antarctica (Retallack and Krull 1999), Coalcliff, Wybung Head, and Frazer Park in Australia (Retallack 1999a), Letham Burn in New Zealand (Waterhouse 1967, 1998; Force 1975; Landis et al. 1999) and Lootsberg Pass, Wapadsberg, and Bethulie in South Africa (Retallack et al. 2003). Flat-pebble conglomerates and claystone breccias at the Permian–Triassic boundary are also known from India (Sarkar et al. 2003), Italy, Iran, Spitsbergen, China, and Canada (Wignall and Twitchett 1999). In all these places, claystone breccias and flat pebble conglomerates contrast with finer-grained overlying and underlying rocks.

Sydney Basin, Australia

The Permian–Triassic boundary in the Sydney Basin of southeastern Australia is at the last appearance of *Glossopteris* leaves, glossopterid chambered roots (*Vertebraria*), and the *Dulhuntyispora* palynozone (Retallack 1995, 1999a), which coincides with a marked carbon isotope anomaly (Morante 1996). The isotopic decline to a minimum is within the last coal formed by *Glossopteris*-dominated swamps: Bulli Coal of Illawarra

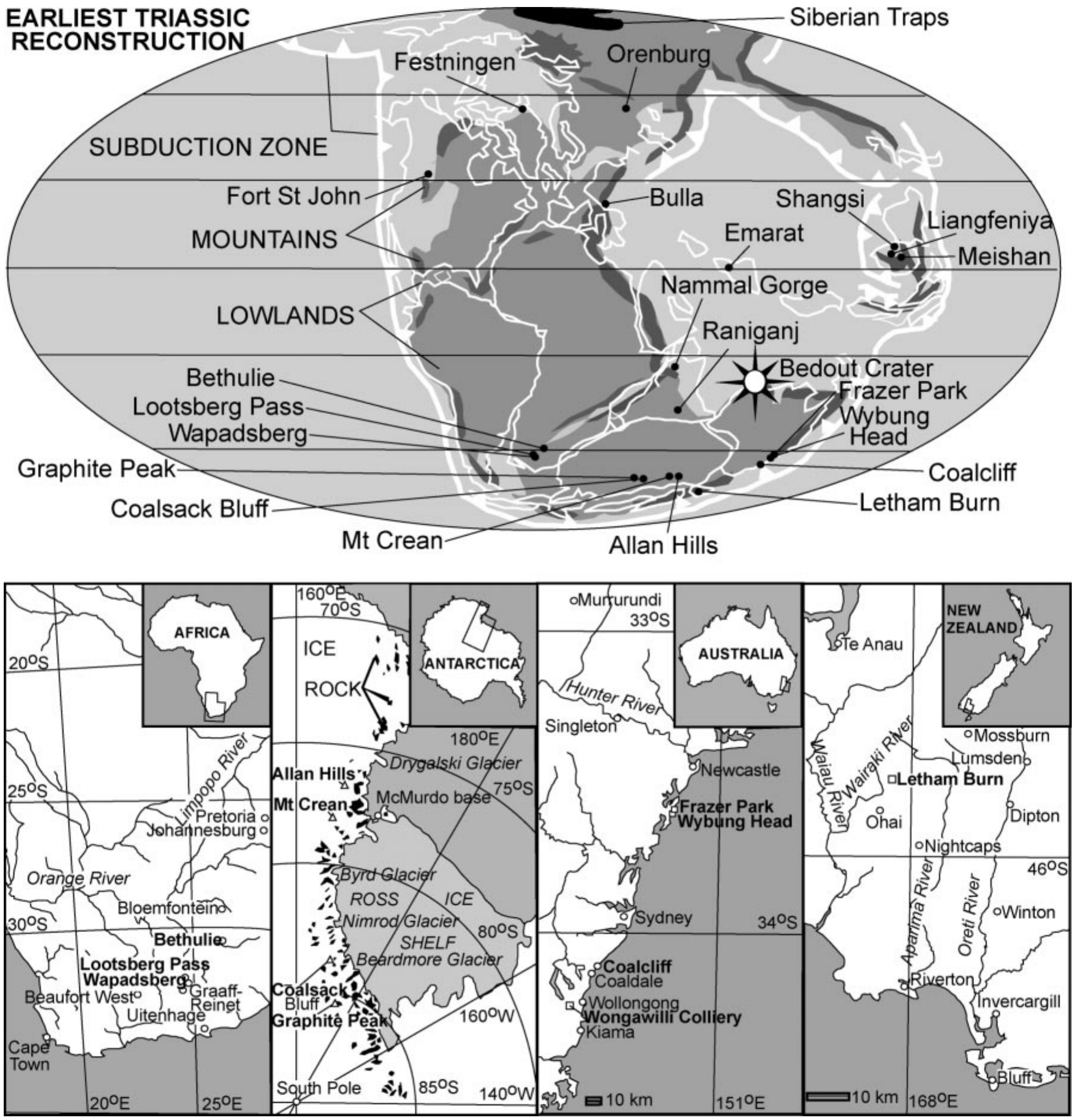

FIG. 1.—Permian–Triassic breccia localities on a continental reconstruction for that time (after Scotese 2001), with localities described here on selected regional maps.

Coal Measures in the southern Sydney Basin, Vales Point Coal of Newcastle Coal Measures to north, and Katoomba Coal of Farmers Creek Formation to the west (Retallack 1999a). This coal is abruptly overlain by channel sandstones and conglomerates of the Narrabeen Group in most places: Coal Cliff Sandstone to south, Dooralong Shale to north, and Widden Brook Conglomerate to west. At some localities, however, there is a meter of shale and claystone below the earliest Triassic paleochannels with a distinctive paleosol (Wybung pedotype of Retallack 1999a). The paleosol and associated shales contain an earliest Triassic fossil flora dominated by *Lepidopteris callipteroides* and a distinctive palynoflora (Retallack 1995, 1997b, 2002b). The earliest Triassic paleosol is developed on a distinctive claystone breccia, which unconformably overlies the last coal (Fig. 2C). These claystone breccias were studied in detail at Coalcliff (E150.96667° S34.25010°) on the coast south of Sydney, as well as at Wybung Head (E151.61901° S33.19948°) and Frazer Park (E151.62701° S33.18874°), which are only 2 km apart on the coast north of Sydney (Fig. 1).

At Wybung Head the claystone breccia pinches out laterally within 4 m from a maximum thickness of 15 cm, with little erosion of the underlying coal, and local thickening and thinning (Fig. 3B). Some depositional partings extend eastward from the claystone breccia into laterally equivalent siltstones below the Wybung paleosol, within a sea cave eroded from a dolerite dike. At Frazer Park the claystone breccia is 20 cm thick by the track on the headland, but both the breccia and Wybung paleosol are cut out completely by a basal Triassic sandstone paleochannel 200 m to the north, beside the parking lot higher on the headland. At the old mine adit at Coalcliff, the Wybung paleosol underlies a cliff-forming paleochannel sandstone and was formed on 12 cm of claystone breccia. Only 50 m to the south around the sea cliffs, the paleosol and breccia are eroded away, and a sandstone paleochannel directly overlies the last coal. In the roof of Wongawilli Colliery 10 km southwest of Wollongong, claystone breccias appear partly crusted and are disrupted by silt-filled mud cracks extending 5–10 cm down into the underlying Bulli Coal (Diessel 1992, p. 201).

Claystone breccias from all the Sydney Basin localities are massive to crudely bedded, with a suggestion of imbrication, in part from the burial

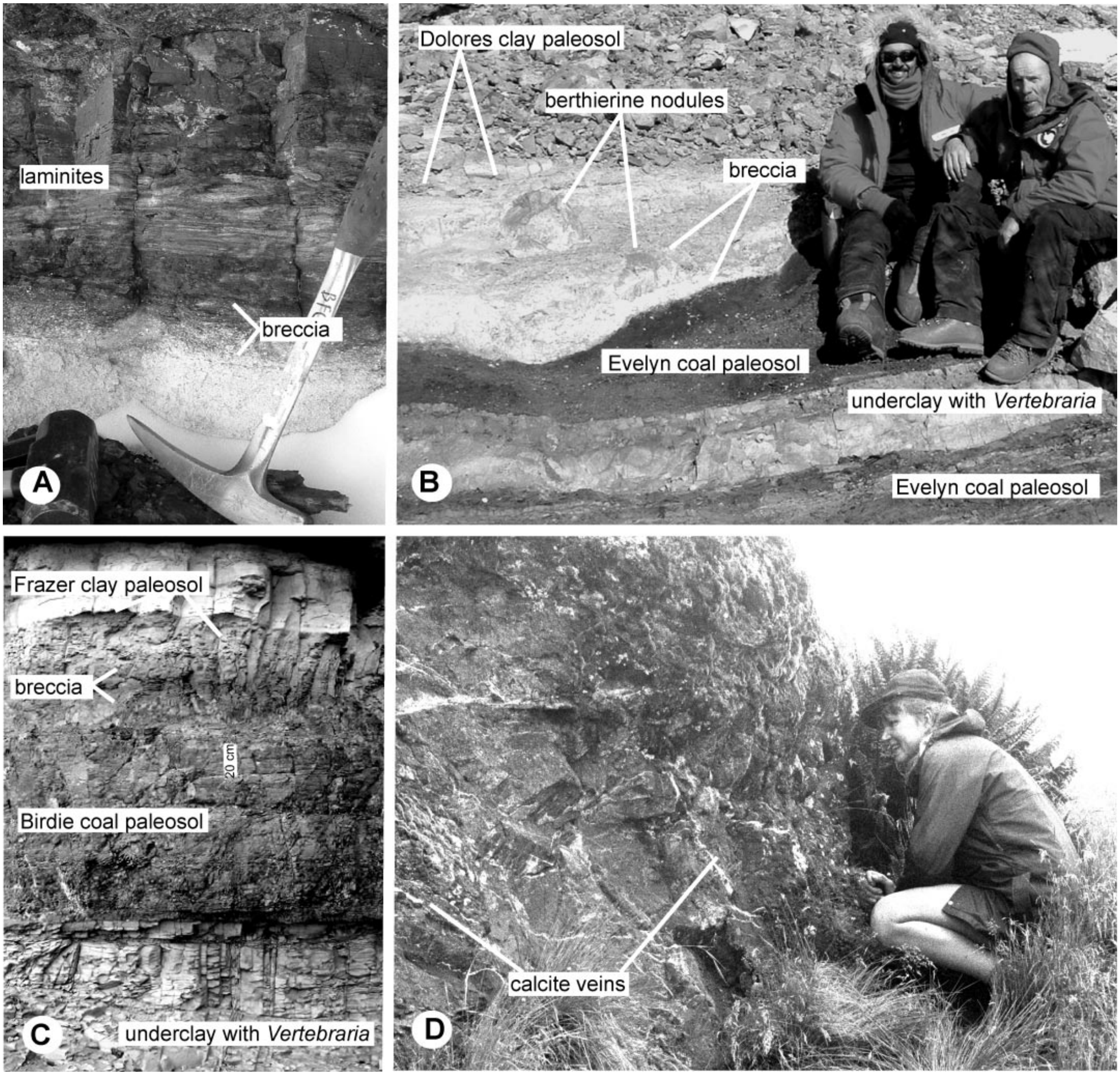

FIG. 2.—Field photographs of claystone breccias at the Permian–Triassic boundary at **A)** Mt Crean, southern Victoria Land, **B)** Graphite Peak, central Transantarctic Mountains, **C)** Wybung Head, northern Sydney Basin, Australia, and **D)** Productus Creek, New Zealand. The thick, tectonically deformed, marine Wairaki Breccia in New Zealand contrasts with thin, channelized, nonmarine claystone breccias in Australia and Antarctica. Hammer for scale in Part A, Ramananda Chakrabarti and Shaun Norman in Part B, 20 cm card in Part C, and Evelyn Krull in Part D. Photos A and B courtesy of Shaun Norman, and Photo C courtesy of Christian Heine.

compaction of claystone clasts (Fig. 4B). The breccias are black to dark gray in color, because they contain abundant clasts of coal and carbonaceous shale (Fig. 4B). In petrographic thin section, clasts of coal and carbonaceous shale form a pseudomatrix surrounding grains of quartz and biotite (Tables 1, 2). In soil terminology (Soil Survey Staff 1999), they are dominated by histic clasts. The Frazer Park and Wybung Head claystone breccias also include clasts with what Brewer (1976) terms mosepic plasmic fabric (Fig. 5E, H) similar to that of the underclay to the coal (Fig. 5A). Some claystone clasts are surrounded by clay skins (argillans of Brewer 1976) of pedogenic origin. Isolated argillans showing ductile deformation (Fig. 5H) are similar to clay skins found in the underlying Birdie paleosol (Retallack and Krull 1999).

In chemical composition, the claystone breccia of Wybung head is very deeply weathered (Tables 3, 4). Its alumina/base molar ratio is in excess of 30, which is exceptionally base-depleted. Low soda and moderate barium/strontium ratio of 4 also indicate deep weathering (compare values of

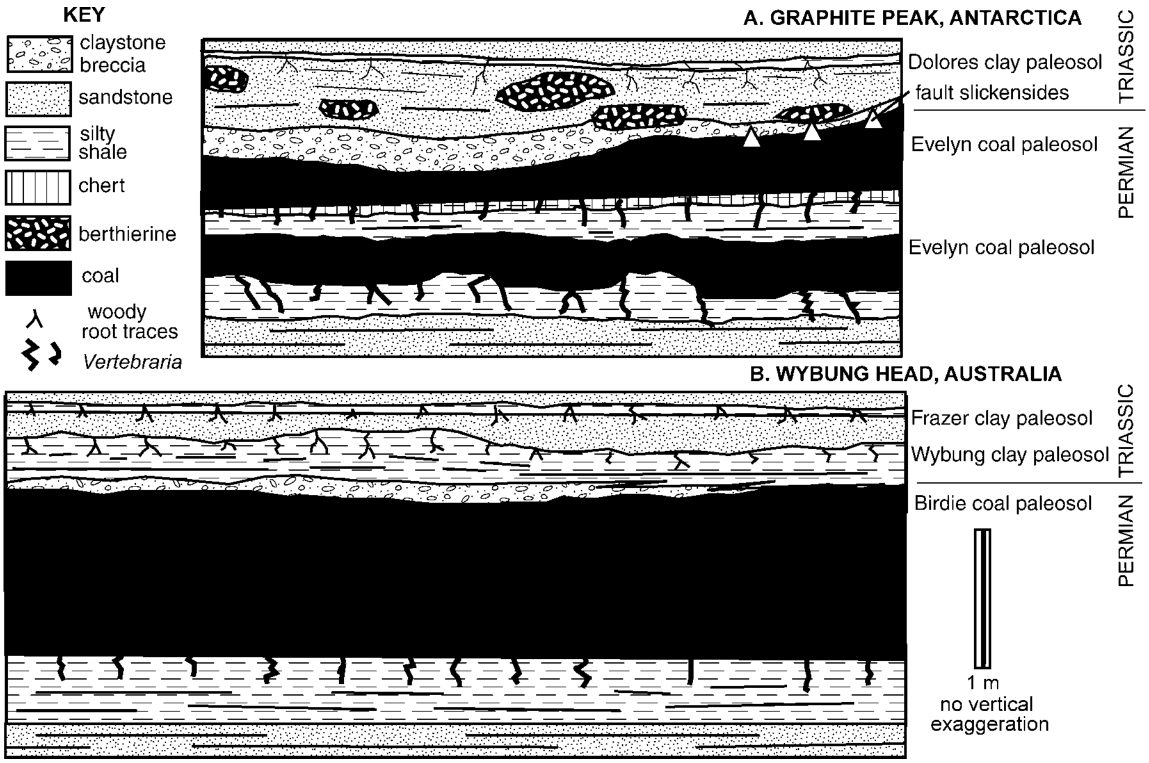

FIG. 3.—Outcrop maps of claystone breccias at the horizon of carbon isotopic perturbation taken to be the Permian–Triassic boundary at **A)** Graphite Peak, central Transantarctic Mountains, and **B)** Wybung Head, northern Sydney Basin, Australia.

Retallack 1997a). Deep weathering also is indicated by clay minerals dominated by kaolinite, with lesser illite and only traces of smectite (Retallack et al. 1998).

Victoria Land, Antarctica

The Permian–Triassic boundary in Victoria Land is also recognized from a carbon isotope anomaly (Retallack et al. 2005) and the last appearance of *Glossopteris, Vertebraria,* and coal as much as 12 m below the contact between Weller Coal Measures and the overlying Feather Conglomerate (Retallack and Krull 1999). The earliest Triassic part of the Weller Coal Measures is not preserved at some localities, such as Portal Mountain, because of eroison by paleochannels of the basal Feather Conglomerate (J.L. Isbell and Cuneo 1996). Where preserved, the earliest Triassic Weller Coal Measures contains Dolores pedotype paleosols, noncarbonaceous root traces, very low organic-carbon contents, and low carbon isotope values, quite unlike the Late to mid-Permian lower part of the coal measures (J.L. Isbell et al. 1999; Retallack et al. 2005). Fossil plants and palynomorphs indicate a late Early Triassic age of the upper Feather Conglomerate (Retallack and Krull 1999).

The claystone breccia at Mt Crean (E159.53333° S77.87383°) commands attention in the field because it appears as if the large white quartz granules are floating in a matrix of black claystone (Figs. 2A, 4A). What appears to be a grain-size anomaly for hydrodynamic sorting is resolved on examination of thin sections, which show that the black clay is a pseudomatrix of compactionally deformed carbonaceous claystone clasts also up to granule size (Fig. 5F; J.L. Isbell et al. 1999, fig. 1). The claystone breccia here is stratigraphically near the top of the Permian Weller Coal Measures, overlain by 21 cm of gray, carbonaceous, silty laminite, and then massive sandstones of the overlying Feather Conglomerate (Retallack and Krull 1999). A shift to lower isotopic values of organic carbon ($\delta^{13}C_{org}$) at the level of the claystone breccia at Mt Crean suggests that it is at the Permian–Triassic boundary (Retallack et al. 2005). The Mt Crean claystone breccia is dominated by opaque claystone clasts rich in organic matter (Table 2). These histic clasts (of Soil Survey Staff 1999) are like those of coals and underclays of the underlying Weller Coal Measures. Other grains in the breccia include quartz granules, hornblende grains, and books of kaolinite (Table 2). Large grains with weathering rinds (diffusion sesquans of Brewer 1976) reflect a period of prior weathering, presumably in soils of local granitic basement rocks of a hilly source land. The chemical composition of this claystone breccia (Tables 3, 4) indicates moderate chemical weathering, with low soda and high barium/strontium ratios comparable with those produced by podzolization (Retallack 1997a). This also is indicated by their clay-mineral composition: largely illite, with small amounts of smectite and kaolinite (Retallack et al. 1998).

Claystone breccia also has been found in the Allan Hills (E159.73623° S76.70240°) in a sandstone matrix immediately below the lowest Dolores paleosol, here taken as earliest Triassic, in the Weller Coal Measures 12 m below the top of its contact with the overlying Feather Conglomerate (Retallack and Krull 1999). Clasts of the Allan Hills claystone breccia are up to 6 mm in size, white and light gray, and mainly mosepic (in the sense of Brewer 1976), like underclays to Evelyn paleosols lower in the same sequence.

Central Transantarctic Mountains

The Permian–Triassic boundary in the central Transantarctic Mountains is marked by a decline in organic-carbon content and carbon isotope values (Krull and Retallack 2000), extinction of *Glossopteris* and *Vertebraria* (Retallack and Krull 1999; McManus et al. 2002) and its palynoflora (Farabee et al. 1991), and appearance of Early Triassic vertebrates *Lystrosaurus murrayi* and *Thrinaxodon liorhinus* (Colbert 1974; Retallack and Hammer 1998; Retallack et al. 2005). The boundary is at the contact between coal measures of the Buckley Formation and green siltstones of the Fremouw

TABLE 1.—*Grain size of Permian-Triassic boundary breccias.*

Locality	Specimen	% Clay	% Silt	% Sand	% Gravel
Frazer Park	R2860	34.2	15.4	18.8	31.6
Wybung Head	R1667	24.8	20.0	26.0	29.2
Coalcliff	R1687	21.4	11.8	12.2	54.6
Allan Hills	R1740	28.8	25.8	26.6	18.8
Mount Crean	R1938	27.2	21.8	26.2	24.8
Graphite Peak	R2060	26.0	14.4	19.0	40.6
Wapadsberg	R2748	30.8	29.0	25.2	15.0
Lootsberg Pass	R2778	27.2	39.6	30.4	2.8
Bethulie	R2823	28.2	30.2	24.0	17.2
Letham Burn	R1592	25.4	12.2	16.2	46.2

Note: Based on 500-point counts using a Swift automatic point counter.

Formation (Collinson et al. 1994), and also is at the level of extinction of all Permian paleosol pedotypes, and first appearance of characteristic Triassic paleosols with noncarbonaceous root traces such as the Dolores pedotype (Retallack and Krull 1999).

The claystone breccia at Graphite Peak (E172.36832° S85.05211°) is a distinctive light olive bed overlying the last thick coal seam of the Buckley Formation and forming the base of the first green paleosol (Dolores pedotype) of the Fremouw Formation (Retallack and Krull 1999). These beds are not naturally exposed, but were excavated and swept clean from under a mantle of loose colluvium. The southern end of the excavated claystone breccia is slickensided and microfaulted at a high angle (dip 82°S on strike 60° magnetic) to these gently dipping rocks (dip 18°S on strike 36° magnetic). In the central part of the excavated area, claystone breccia fills a narrow (1.8 m wide by 42 cm deep) paleogully (Figs. 2B, 3A). In a second area cleared of scree some 200 m along strike to the south, neither the claystone breccia nor coal were found, but rather paleochannel sandstones with a thin (13 cm) vein of microspherulitic prehnite (Retallack 1999b). The prehnite dike is an extension of a nearby dike of intrusive Ferrar Dolerite, which may have coked the coal at this stratigraphic level along strike (Retallack and Krull 1999, fig. 3). In addition to intrusive destruction of the coal, this dominantly sandstone sequence may reflect earliest Triassic erosion of claystone breccia and much coal.

The Graphite Peak claystone breccia is dominated by noncarbonaceous claystone clasts with wispy intersecting streaks of highly birefringent oriented clays of the kind called by soil micromorphologists mosepic plasmic fabric (Fig. 5C, D). These grains also show thick weathering rinds (Fig. 5C, D), or diffusion sesquans of Brewer (1976). Other grains have relict crystal outlines and appear to be weathered basaltic–andesitic rock fragments. In hand specimen, volcanic clasts are subangular, dark, and hard, whereas sepic claystone clasts have angular to ragged margins and are soft and off-white (Fig. 4C). Sepic claystone clasts are texturally similar to paleosols of the underlying Permian Buckley Formation (especially Molly pedotype, Fig. 5B). Coal and carbonaceous shale clasts are present, but rare (only 0.4%, counted within isotic grains of Table 2). The degree of chemical weathering of this claystone breccia is weak (Tables 3, 4), as indicated

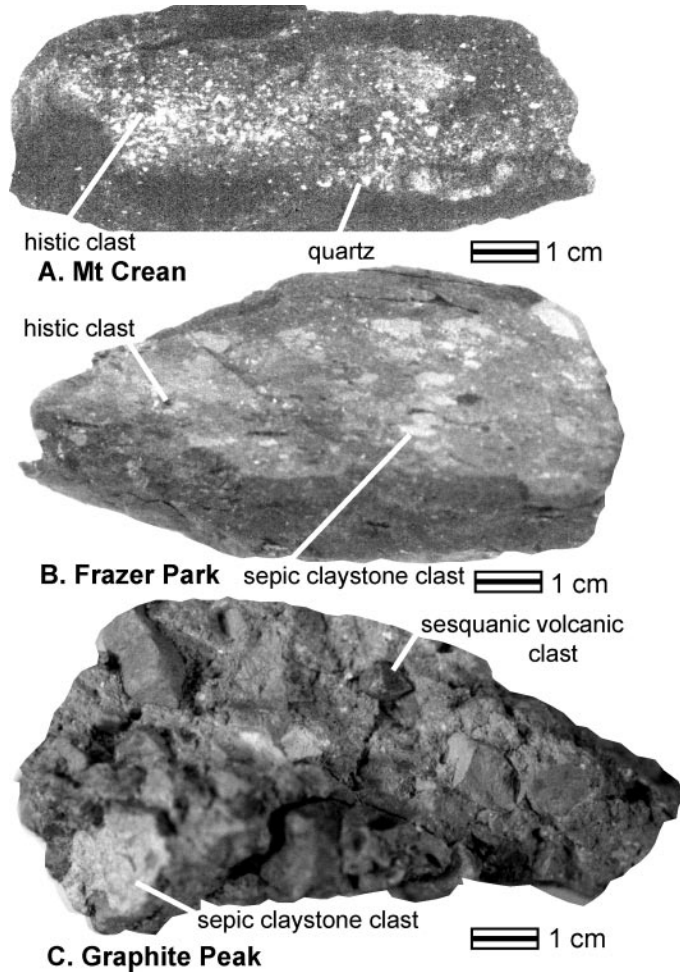

FIG. 4.—Hand specimens of claystone breccias at the horizon of carbon isotope perturbation taken to be the Permian–Triassic boundary at **A)** Mt Crean, southern Victoria Land, **B)** Frazer Park, northern Sydney Basin, Australia, and C) Graphite Peak, central Transantarctic Mountains.

by low alkali and alkaline earth content and by illite–smectite composition (Retallack et al. 1998).

At Coalsack Bluff (E172.29979° S84.23989°), the highest thick, coaly, Evelyn paleosol is overlain by sandstones dark with coal and carbonaceous shale (histic) clasts, and strongly pyritized at the top. Claystone breccia is 15 cm thick and grades up into 70 cm of sandstone capped by another 10 cm of black claystone breccia, which is 10 m below the first Dolores paleosol of the Fremouw Formation (Retallack et al. 2005).

TABLE 2.—*Petrographic composition of Permian-Triassic boundary breccias.*

Locality	Specimen	Clay	Mafic	Feld.	Mica	Bryo.	Calcite	Calcic	Crystic	Masepic	Mosepic	Insepic	Sesquanic	Lithic	Isotic	Qtz
Frazer Park	R2860	34.8	1.0	7.8	1.8	0	0	0	0	2.2	5.6	3.8	2.8	2.8	20.6	16.8
Wybung Hd	R1667	24.8	0.4	5.2	10.2	0	0	0	0	2.4	4.8	10.2	1.4	1.6	23.2	15.8
Coalcliff	R1687	22.2	1.8	8.2	2.0	0	0	0	0	1.6	1.6	2.6	7.2	1.2	40.0	11.6
Allan Hills	R1740	28.8	1.4	23.3	8.6	0	0	0	0	1.2	0.8	2.6	3.4	2.2	1.8	26.0
Mt Crean	R1938	27.0	0.6	10.2	18.6	0	0	0	0	0	0	0	2.2	3.2	17.8	20.4
Graphite Pk	R2060	25.0	2.8	9.4	3.0	0	0	0	0	5.0	6.2	11.8	3.8	3.6	4.8	24.6
Wapadsberg	R2748	30.4	1.2	14.8	5.2	0	3.8	9.2	1.2	0.4	1.4	0.6	1.0	2.0	11.8	16.8
Lootsberg P.	R2778	27.8	1.2	11.0	2.6	0	3.8	12.4	0.4	0	0.8	7.8	1.6	3.4	12.8	14.4
Bethulie	R2823	27.0	1.8	10.2	4.2	0	2.0	10.8	0.4	0	0.4	7.6	2.2	2.2	17.6	13.6
Letham Burn	R1592	26.8	3.0	10.0	1.2	2.8	4.6	0	0	0	0	0	23.4	12.0	15.8	0

Note: Based on 500-point counts using a Swift automatic point counter. Abbreviations include Feld. (feldspar crystals), Bryo. (stony bryozoan fragments), and Qtz (quartz). Calcite is sparry calcite, whereas calcic are micritic, pedogenic carbonate rock fragments. Isotic includes opaque minerals as well as fragments of peat and carbonaceous shale. Mafic minerals are mainly hornblende, but amphibole and pyroxene at Letham Burn.

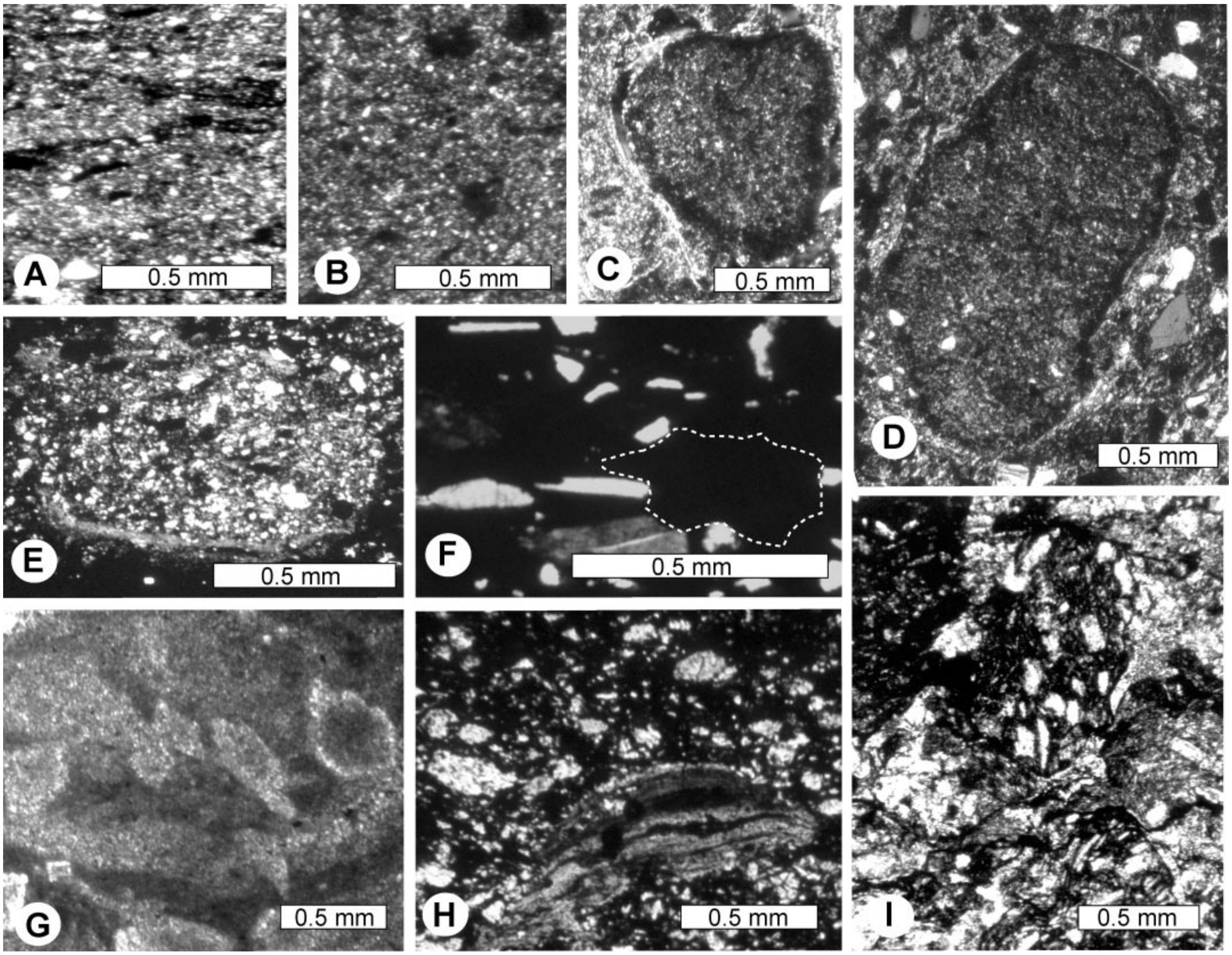

FIG. 5.—Petrographic appearance of latest Permian paleosols (A, B) compared with clasts in earliest Triassic claystone breccias (C–I; all under crossed nicols): **A)** insepic plasmic fabric and root traces in surface horizon (underclay) of type Birdie paleosol from Wybung Head, Australia; **B)** mosepic plasmic fabric in surface horizon of type Molly paleosol from Graphite Peak, Antarctica; **C, D)** mosepic claystone clasts with diffusion sesquan from earliest Triassic claystone breccia at Graphite Peak, Antarctica; **E)** insepic claystone clast with marginal argillans from earliest Triassic claystone breccia at Frazer Park, Australia; **F)** opaque carbonaceous (histic) claystone clasts forming a pseudomatrix to quartz granules in the earliest Triassic claystone breccia at Mt Crean, Antarctica; **G)** pedogenic caliche with evaporitic pseudomorphs (calcic and crystic clasts) in earliest Triassic claystone breccia at Bethulie, South Africa; **H)** mosepic claystone clasts and large clay-skins (argillans) in earliest Triassic claystone breccia at Wybung Head, Australia; **I)** volcanic grains with opaque weathering rinds (sesquans) in a calcite matrix of latest Permian Wairaki Breccia, Letham Burn, New Zealand. Scale bars are 0.5 mm, and all thin sections were cut perpendicular to bedding.

Karoo Basin, South Africa

The Permian–Triassic boundary in the central Karoo Basin of South Africa is defined biostratigraphically by the extinction of vertebrates of the *Dicynodon* zone, and survival of a depauperate fauna of *Lystrosaurus, Micropholis, Proterosuchus,* and *Galesaurus* within the Palingkloof Member of the Balfour Formation, below massive sandstones of the Katberg Formation (Smith and Ward 2001). This placement of the boundary is supported by magnetostratigraphy (Ward et al. 2005), the onset of several negative carbon isotope anomalies found in organic carbon, pedogenic carbonate carbon, and therapsid-tusk-enamel carbon (MacLeod et al. 2000; de Wit et al. 2002), and a pronounced sulfur isotopic anomaly (Maruoka et al. 2003). Latest Permian paleosols are very distinct from earliest Triassic paleosols and separated from them by a widespread and thick (7 m) sequence of laminites, which appear to be lacustrine in origin (Retallack et al. 2003). In KwaZulu-Natal, northeast of the most productive vertebrate beds, a latest Permian flora with *Glossopteris, Lidgettonia,* and *Vertebraria* in coal measures of the Estcourt Formation disappears at the unconformable boundary with the Katberg Formation, which contains *Lystrosaurus murrayi* and *Thrinaxodon liorhinus* (Anderson and Anderson 1985).

Claystone breccias at the Permian–Triassic boundary were examined in the creek below Lootsberg Pass (E24.870767° S31.850867°), on the road pass over Wapadsberg (E24.885636° S31.902314°), and in a creek east of Bethulie (E26.2689330° S30.422467°). All three have clasts predominantly of calcareous nodules (Table 2), identical to calcic horizons (of Soil Survey Staff 1999) in underlying Som and Bada paleosols (Retallack et al. 2003), and often rusty with ferruginous weathering rinds on the clasts (diffusion sesquans of Brewer 1976). At Bethulie and Wapadsberg a few of the clasts contain silicified pseudomorphs of evaporitic minerals such as gypsum (Fig. 5G). At Lootsberg Pass, a few clasts are red claystone with insepic fabric like that in Zam paleosols of the underlying laminites (Retallack et

TABLE 3.—*Chemical composition of Permian-Triassic boundary breccias.*

Locality	Specimen	SiO_2	TiO_2	Al_2O_3	Fe_2O_3	FeO	MnO	MgO	CaO	Na_2O	K_2O	P_2O_5	Ba	Sr	LOI	Total
Wybung Hd	R1667	44.46	2.07	23.93	0.40	0	0	0.14	0.04	0.10	0.19	0.01	129	21	28.74	100.09
Mt Crean	R1938	30.78	0.80	13.32	<.01	0.75	<.01	0.23	0.34	<.01	2.66	<.03	946	70	49.27	98.17
Graphite Pk	R2060	64.02	0.82	17.82	3.62	0.13	0.05	0.89	1.53	0.17	2.56	0.06	455	167	8.68	100.30
Lottsberg P.	R2778	35.41	0.29	7.44	1.79	0	1.39	0.65	26.81	1.49	1.45	0.13	253	273	22.28	99.20

Note: Analyses are weight percent for oxides but ppm for Ba and Sr, from inductively coupled plasma-atomic fusion by Bondar Clegg Inc, Vancouver. Errors were estimated from standards of 1989 CANMET SY-3 and CANMET SO-2 for ICP.

al. 2003, fig. 3C). Clay minerals in Lootsberg and Wapadsburg claystone breccias are mainly illite–smectite, with small amounts of kaolinite. The chemical composition of the calcic pedolith at Lootsberg Pass (Tables 3, 4) shows little chemical weathering, and evidence of a calcic and sodic soil source (Tables 3, 4).

Letham Burn, New Zealand

Latest Permian age of the Wairaki Breccia in the Taringatura Hills of New Zealand is inferred largely from its fossil fauna of brachiopods of the *Wairakiella rostrata* zone (Waterhouse 1967, 1998). Geological mapping of the area shows a general sequence from western mid-Permian marine limestones to eastern early Triassic conglomerates, though disrupted by stacked thrust faults (Force 1975; Waterhouse 1998; Landis et al. 1999). Continuous stratigraphic sections have not been measured because of structural complications and poor exposure.

This study focused on large outcrops above steep slopes and cliffs of Glendale Limestone on the southern slopes of Alec Mutch Creek, the first tributary of Letham Burn above its confluence with the Wairaki River (Fig. 1: S45.77535° E167.95200°). The outcrop exposes thick-bedded, poorly stratified granule breccia, with partings and tension gashes filled with calcite (Fig. 2D). The breccia clasts are mostly rounded granules of basaltic–andesitic lava, like those of the earlier Permian volcanics in the Old Wairaki Hut Formation (Waterhouse 1998). In thin section, many of these clasts show complete or marginal ferruginization (diffusion sesquans of Brewer 1976). The matrix in thin section is largely sparry calcite, which supports the delicate structures of latest Permian stony bryozoans (*Dyscritella* sp.).

Other Earliest Triassic Breccias and Conglomerates

Flat-pebble conglomerates are a distinctive coarse-grained facies of many Permian–Triassic supratidal and intertidal sequences in Canada (Fort St John), Spitsbergen (Festningen), Italy (Bulla), Iran (Emarat), Pakistan (Nammal Gorge), and China (Lianfeniya and Shangsi) (Baud et al. 1989; Davies et al. 1997; Wignall and Twitchett 1999). I have also seen flat-pebble conglomerates in earliest Triassic tidalite facies of the Chinlung Formation at the Xujiashan cement factory, 15 km east of Nanjing, China (approx. E118.96° N32.05°). Wignall and Twitchett (1999) interpret these as tempestites from tidal flats dominated by cyanobacteria, comparable to those widespread in late Precambrian and Cambrian intertidal and shallow marine strata (Sepkoski 1982). The abundance of stromatolites and calcimicrobial carbonates at the Permian–Triassic boundary is another indication of conditions comparable to those of the earliest Paleozoic (Schubert and Bottjer 1992; Lehrmann et al. 2003).

Nonmarine breccias at the Permian–Triassic boundary also include the Clayey Sandstone Member of the Nordhausen Formation of the Thuringian Basin of Germany (Kozur 1993), and the uppermost Raniganj Coal Measures, near Banspetali, India (Sarkar et al. 2003). Other examples are thin conglomerates within laminites near Orenburg, Russia (Benton 2003, p. 244), in a stratigraphic sequence of laminites between fluvial facies very similar to that in the Karoo Basin of South Africa, which yielded the calcic pedoliths described here.

TABLE 4.—*Molar weathering ratios of Permian-Triassic boundary breccias.*

Locality	Specimen	Alumina/ Bases	Soda/ Potash	Barium/ Strontium
Wybung Hd	R1667	30.03	0.80	3.92
Mt Crean	R1938	3.25	0.01	8.62
Graphite Pk	R2060	2.20	0.10	2.44
Lootsberg P.	R2778	0.14	1.56	0.59

Note: These calculations and their interpretation are explained by Retallack (1997a).

COMPARABLE MODERN SEDIMENTS IN OREGON

There is no perfect modern analog for the Permian–Triassic life crisis, thank goodness, but much can be learned by seeking situations where soils are freshly eroded. Among the various kinds of paleosol fragments recognized in earliest Triassic claystone breccias, ferruginized clasts are widespread in areas of current or former tropical soils (Retallack 1991). Most channels and gullies in aridlands contain lag concentrations of pedogenic calcareous nodules (Tandon and Narayan 1981). In contrast, sepic clasts are rare and hard to find in sediments. In the field, these can be identified by abundant brown or gray granules, easily crushed between the fingers, and workable into a clay pellet. I have found them only associated with road construction and clear-cut logging in the Coast Range and Cascades foothills near Eugene, Oregon (Fig. 6). This is a hilly region largely given over to commercial forestry based on Douglas fir (*Pseudotsuga menziesii*) in a humid, summer-dry, cool temperate climate (Swanson and Dyrness 1975; Swanston and Swanson 1976; Grant and Wolff 1991; Rosenfeld 2000). Eugene in the period 1951–1977 had a mean annual precipitation (MAP) of 1114 mm, with 226 mm in January and 6 mm in July, and a mean annual temperature (MAT) of 11.4°C (Patching 1987). This is comparable with paleoclimate estimated using geochemical transfer functions (Sheldon et al. 2002) from earliest Triassic paleosols at Wybung Head (1478 ± 235 mm MAP, 14.9 ± 4.4°C MAT; Retallack, 1999a), Allan Hills (1434 ± 235 mm MAP, 13.4 ± 4.4°C) and Graphite Peak (1148 ± 235 mm MAP, 12.8 ± 4.4°C MAT: Retallack and Krull 1999), but not Lootsberg Pass (801 ± 235 mm MAP, 14.9 ± 4.4°C: Retallack et al. 2003), where redeposited soil clasts were calcic and crystic rather than sepic.

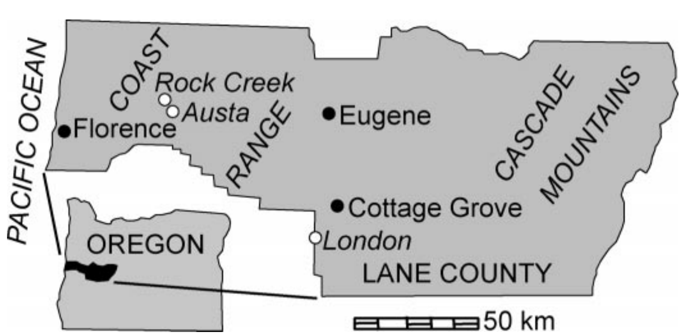

FIG. 6.—Modern pedolith sites examined in the Oregon Coast Range and Cascades.

Field Observations

Three recently exposed soils were visited and sampled for petrographic and particle-size analysis. The Rock Creek site on 9 February, 2003 was a miniature (30 cm wide and 20 cm high) talus cone within a backhoe ditch excavated in January 2003, to block vehicular access to a ridge-top power-line access road 2 km northwest of Austa, in the Coast Range of Lane County, Oregon (W123.669583° N44.026500°). This talus cone had the appearance of dry ravel deposits, common in this area after forest fires (Gabet 2003; Wondzell and King 2003). The sediments were cut with a machete and pressed into a 1 × 4 × 5 cm tin (purchased with Altoids® peppermints) for later thin-section preparation. These samples came from the bottom of the backhoe trench, 1.5 m below road level at a point 2 m below a road cut exposing a thick soil (Bohannon gravelly loam, Haplumbrept of Patching 1987). The layered breccia of this small (20 cm high by 25 cm wide) talus cone includes (1) deeply weathered, yellow fragments of Eocene Tyee Formation from the C horizon of the soil exposed in the saprolite, (2) highly ferruginized fragments of local diabase dikes (Walker and MacLeod 1991), and (3) granule-size, brownish-gray, claystone soil peds, easily crushed between the fingers and soluble in water.

A clear-cut on a gently sloping summit ridge below the main logging road on the ridgetop 1 km north of Austa, also in the Coast Range of Lane County, Oregon (W123.658200° N44.012283°), was also sampled for thin-sections on 9 February, 2003, in a shallow (6 cm deep by 14 cm wide) rill within the burned area of a slash pile (Fig. 7A, B). This wood lot had been clear-cut in January 2001, with local slash burning and replanting in February 2002. The ground here was puffy with charcoal, and small debris flows (in the sense of Swanson and Dyrness 1975), which were dissected by small rills (Fig. 7A, B). The soil at this site is a Dystrochrept of the Blachly silty clay loam (Patching 1987), developed on fine-grained sandstones of the Tyee Formation (Walker and MacLeod 1991). The ridge-top nearby includes Plio-Pleistocene red gravels (like those described by Parsons 1978), which also could have contributed to this soil by slope wash and creep. Apart from abundant charcoal chips 2–4 mm square, this layered deposit consisted largely of brownish gray claystone granules, which dissolve to a muddy suspension in water and are easily crushed by hand.

Several sampling visits (26 April, 7 and 9 May, and 22 September, 2003) were made to a bulldozed landing for a clear-cut drag line just below the ridge crest west of Cottage Grove Lake and 4 km north of London, in the Cascades foothills of Lane County (N43.68440° W123.136139°). This clear-cut and landing had been completed by Weyerhauser Corporation in February 2003. Successive visits monitored the emplacement and weathering of a series of small mudflows (Fig. 8C–E) from a bulldozed cut exposing late Eocene red paleosols (Retallack et al. 2004), and a modern soil (Argixeroll of Dixonville silty clay loam of Patching 1987). The late Eocene paleosols of the Fisher Formation are sandwiched between underlying late Eocene tuff and overlying late Eocene basalt flows which crop out on the ridge upslope (Retallack et al. 2004). Newly formed mudflows, initiated by individual rainfall events, were small (9.8 and 8.4 cm thick, and 1340 and 120 cm wide, respectively, for two examples) and showed coarse-grained marginal ridges raised 2–3 cm above the central part of the flow at the snout and margins of the mudflow. Subsequent rainfall events dissected the central part of the mudflow by rill erosion, and destroyed many clayey clasts by dissolution in ponded water. Clay settling from the water formed a crust 8–9 mm thick, which was then disrupted slightly by mud cracks if not overrun by a subsequent mudflow (Fig. 7C). After only three months, these surfaces supported herbaceous plants and were unrecognizable as debris flows (Fig. 7E). Erosional gullies were thus filled with a sequence of surficially weathered debris flows, each about 5–10 cm thick, with a clayey and mud-cracked surface crust.

Grain-Size Measurements

Progressive weathering of one debris flow near London was assessed by determination of its grain size 13, 26, and 149 days after it was formed in a rainstorm. These were all samples from within the debris flow, beneath the surface crust in which all clay grains had slaked to clay, sprinkled with silt and sand. Sand and clay proportions were determined by sieving, but grains larger than 2 mm were measured individually using digital calipers. Median grain size decreased through time from 1.41, to 0.95, to 0.58 mm, for 13, 26, and 149 days, respectively (Fig. 8). Decline in the interquartile spread of sizes was more profound, as was the loss of large clayey peds, with none larger than 4 mm surviving more than two weeks.

Petrographic Observations

Thin sections were prepared of sediments at each of the sites, by impregnating with dilute epoxy and grinding under kerosene (Tate and Retallack 1995). A wide array of pedogenic fabrics were observed, even within an individual thin section (Fig. 9A). Most were matrix-poor and uncemented aggregates. Many showed intersecting streaks of highly birefringent clay characteristic of the subsurface clayey (Bt) horizons of well drained soils (Fig. 9B, C; mosepic and masepic of Brewer 1976). Some of these showed remnants of adhering clay skins (argillans of Brewer 1976) from the original soil (Fig. 9B), whereas others were embayed and ragged as if breaking down (Fig. 9C). Many rock fragments, especially of basalt and diabase showed varying degrees of ferruginization, from fresh interiors with thin opaque weathering rinds (Fig. 9D) to grains substantially reddened and rendered opaque by iron oxide (Fig. 9A). Yet other fragments were completely opaque and appear to be iron–manganese soil nodules, sometimes with adhering remnants of soil (Fig. 9E).

Specimens of soil granules from a mudflow only 13 days old near London showed a variety of clayey and organic films, and common fungal hyphae, when examined by scanning electron microscope (Fig. 10). Some of the hyphae were well preserved and abundant (Fig. 10A, C), but in others only collapsed and degraded remnants of hyphae remain on the mud-plastered surface (Fig. 10D). Clay skins on the surfaces of the claystone clasts bear the impressions of a mat of hyphae no longer present, as well as peeling films of organic matter (Fig. 10B). Such a living network of hyphae, as well as organic films and clay skins, are abundant in soils, but rapidly decay on sedimentary clasts.

Point counting of thin sections indicates degradation of some kinds of clasts, but persistence of others in the mudflow near London, sampled 13, 26, and 149 days after it formed (Fig. 11).Pedogenic claystone clasts drop precipitously in abundance after two weeks, even within the part of the mudflow protected by a surface clayey crust. This is especially true of clasts with common highly birefringent clay separations that intersect (masepic) or are just short of intersecting (mosepic of Brewer 1976). Such fabrics are common in the clayey subsurface (Bt) horizon of the surface soil here, whereas less pedogenically modified fabrics of small birefringent streaks (insepic) are found in the deeply weathered saprolite (C horizon) of this soil. In contrast, fresh (lithic of Fig. 11) and oxidized (sesquanic) rock fragments and iron–manganese nodules (isotic) increase in relative abundance as claystone clasts slake in the rain.

Insights from Modern Soil Erosion

In Oregon clearcuts today, clayey soil peds with sepic plasmic fabric are physically fragile and chemically reactive with water, and do not persist at the surface for more than a single heavy rain. Even 5–10 cm below the 8–9-mm-thick surface clayey crusts, claystone clasts are destroyed within a few weeks. None were found within any erosional gullies or creeks of the region, even on very steep slopes such as those above the Siuslaw River immediately north of Austa. Sepic peds can be transported only short distances by mechanisms that do not involve prolonged immersion in water, such as debris flow (Swanson and Dyrness 1975) or dry ravel (Gabet 2003).

These conclusions based on petrographic observations are supported by other studies on soil aggregate stability. Clayey soils vary widely in the

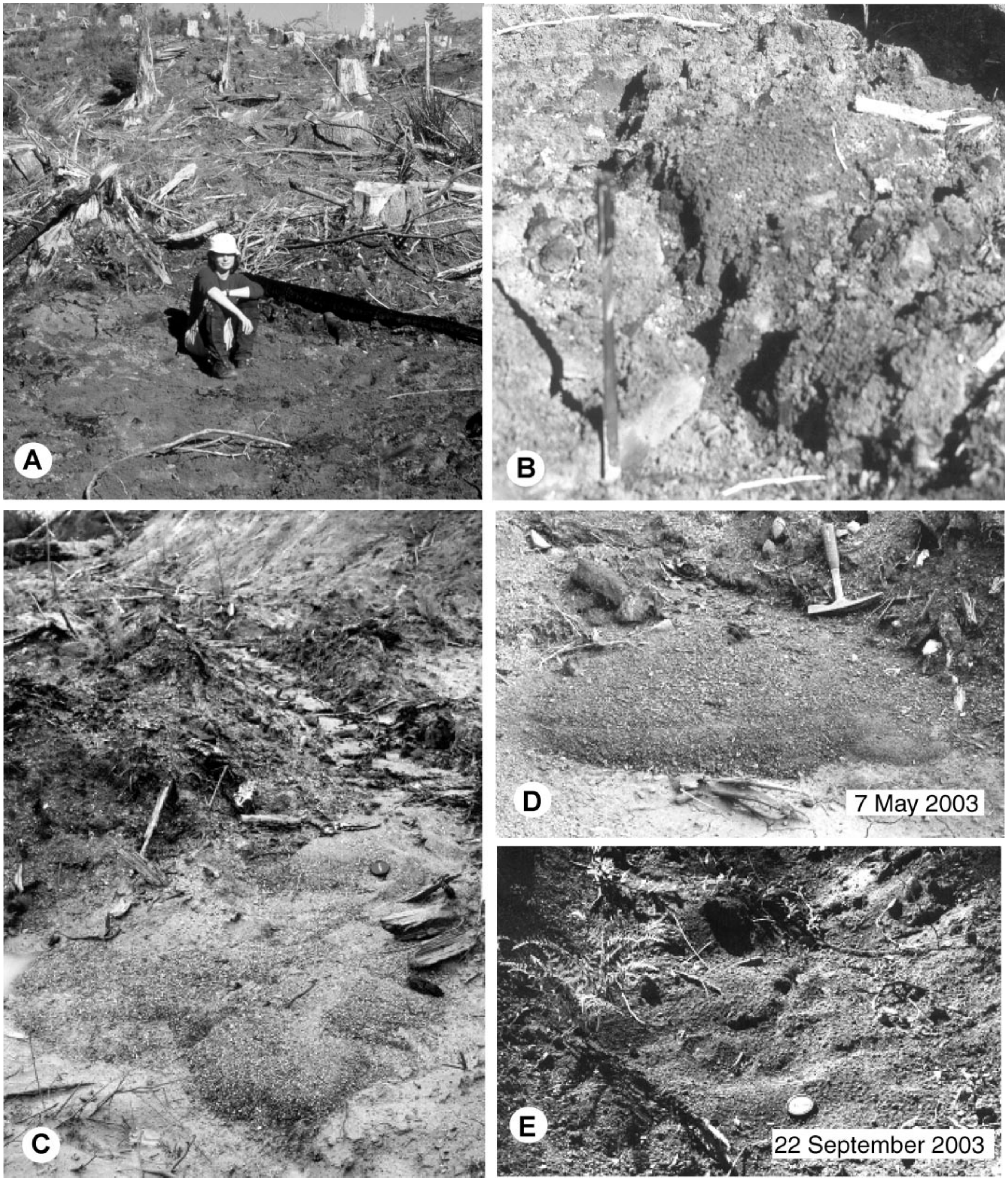

FIG. 7.—Modern pedoliths of Oregon at A, B) Austa clear-cut, showing **A)** bare ground and **B)** rill erosion creating layered pedolithic claystone breccia; and C, D) bulldozed landing for London clear-cut, showing **C)** debris flow of pedolithic claystone breccia from roadside ditch, and **D)** from a nearby low embankment, and **E)** the latter eroded and weathered during a later visit. Scales include Carolyn Phillips in Part A, machete planted by cut though claystone breccia in Part B, 55 mm lens caps in Parts C and E, and hammer in Part D.

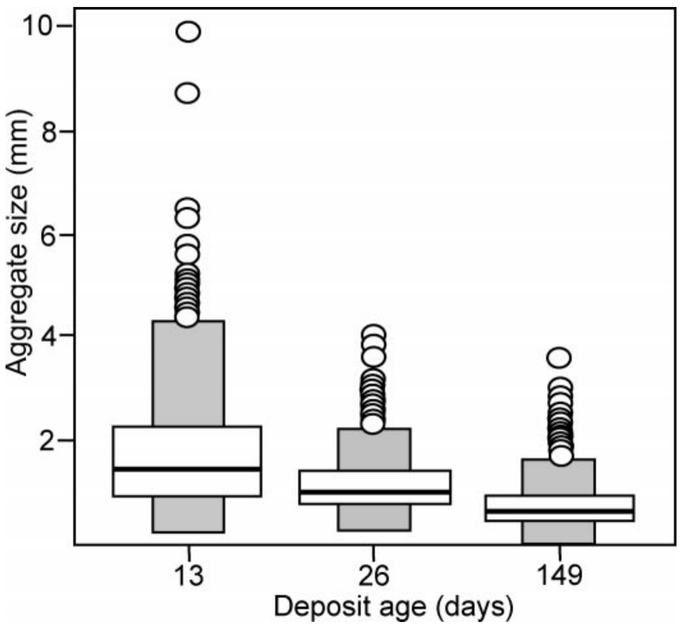

FIG. 8.—Changing grain size through time of a pedolithic debris flow near London, Oregon (Fig. 7C–E). Data are arrayed in quartiles around the median (heavy line), with all grains of the upper quartile plotted (open circles). There is a pronounced reduction in grain size, especially of large soil clasts.

stability of their peds, which can be broken down by slaking in water, by microcracking during differential swelling, by chemical dispersion, and by raindrop impact (Barthes and Roose 2002). Least stable are peds of sodic smectite (rich in exchangeable ionic sodium; Rienks et al. 2000), followed by less sodic smectites (Amezketa et al. 1996). Such soil peds disperse into suspension in water within minutes, sometimes explosively, whereas some kaolinitic peds survive weeks of immersion (Reichert and Norton 1994; Triplehorn et al. 2002). Clayey soil peds are stabilized in soils by roots (Ekanayake et al. 1997; Schmidt et al. 2001), by crop mulch (Sood and Chaudhary 1980), by manure (Pare et al. 1999), by fire-induced hydrophobic aliphatic compounds (D'Acqui et al. 1999), and by silica, carbonate, iron, or aluminum cements (Reichert and Norton 1994; Lindbo and Rhoton 1996; Le Bissonais 1996). Neither a high total clay content nor a high total organic content increase resistance of peds to slaking, so that the quality and external binding location of clay and organic matter is more critical than bulk composition (Rienks et al. 2000; Zhang and Horn 2001). Large peds are less susceptible to slaking than small ones (Shainberg et al. 1997), and angular peds are more susceptible than rounded ones (Manaenkov et al. 1997). Most tests of ped slaking use water, but slaking is more rapid in a solution of 3% acetic acid, further accelerated in 1% NaOH and $K_4P_2O_5$ (Manaenkov et al. 1997), and even faster in surfactants such as hydrazine (Triplehorn et al. 2002). Slaking of soil peds in exposed soils and badlands creates muddy runoff and clayey crusts to the surface of rills, gullies and badlands, and such crusts can impede further slaking (Moore and Singer 1990; Bajracharya and Lal 1998; Faulkner et al. 2003). Nevertheless, crusts are broken by shrinkage of microbial crusts, lichens, and mosses to create popcorn-shaped peds that are easily eroded (Schumm 1962; Engelen 1973). Heavy rainfall leads to massive slaking and large losses of clay in suspension before crusting, but gentle slow rainfall and

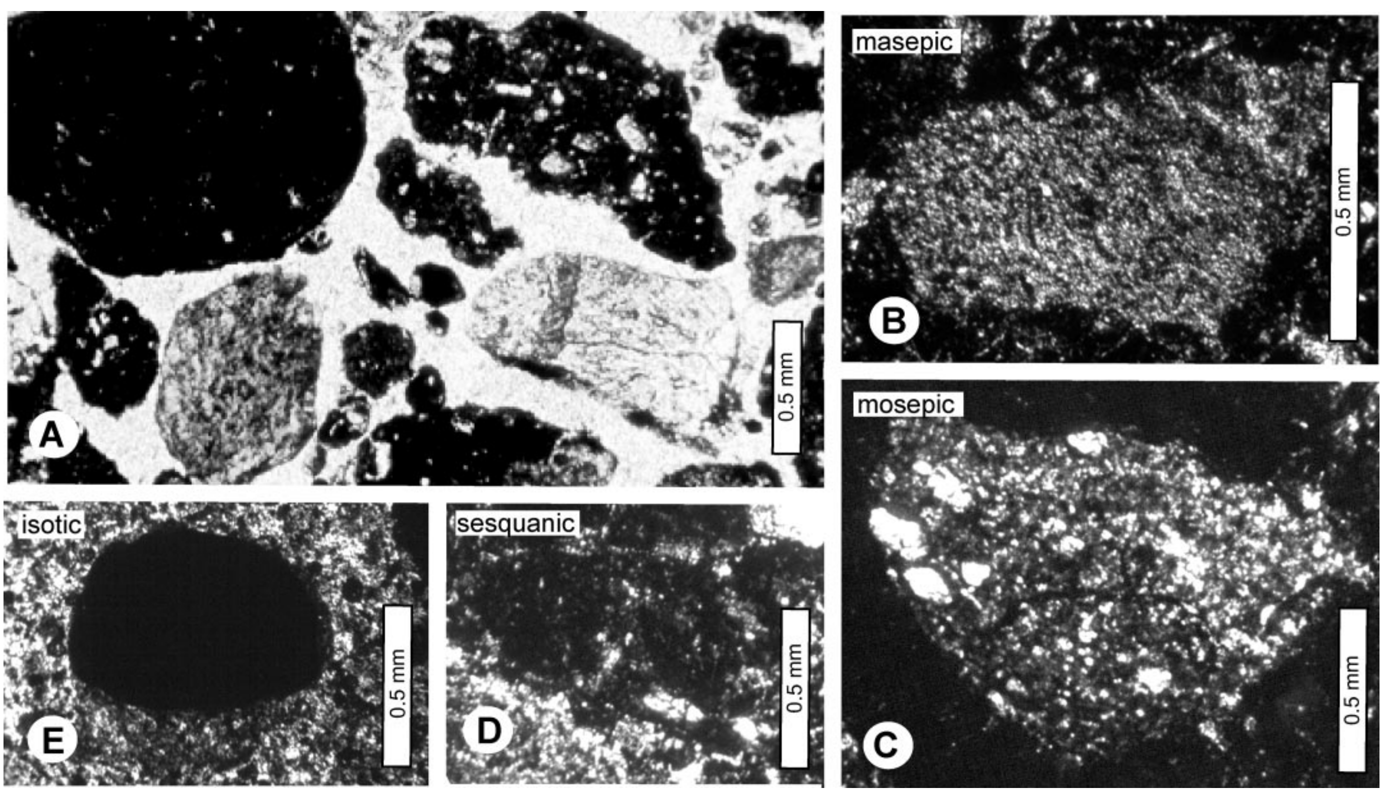

FIG. 9.—Photomicrographs of soil clasts in modern sepic pedoliths from the Oregon Cascades and Coast Range (all viewed under crossed nicols): **A)** masepic, sesquanic, and isotic soil clasts from Rock Creek; **B)** masepic soil clast from Rock Creek; **C)** mosepic weathered basalt with clayey phenocryst pseudomorphs from Austa; **D)** weathered basalt clast with sesquan from Rock Creek; **E)** isotic clast (iron manganese soil nodule) with attached insepic soil matrix (lower meniscus) from Austa. Scales all 0.5 mm.

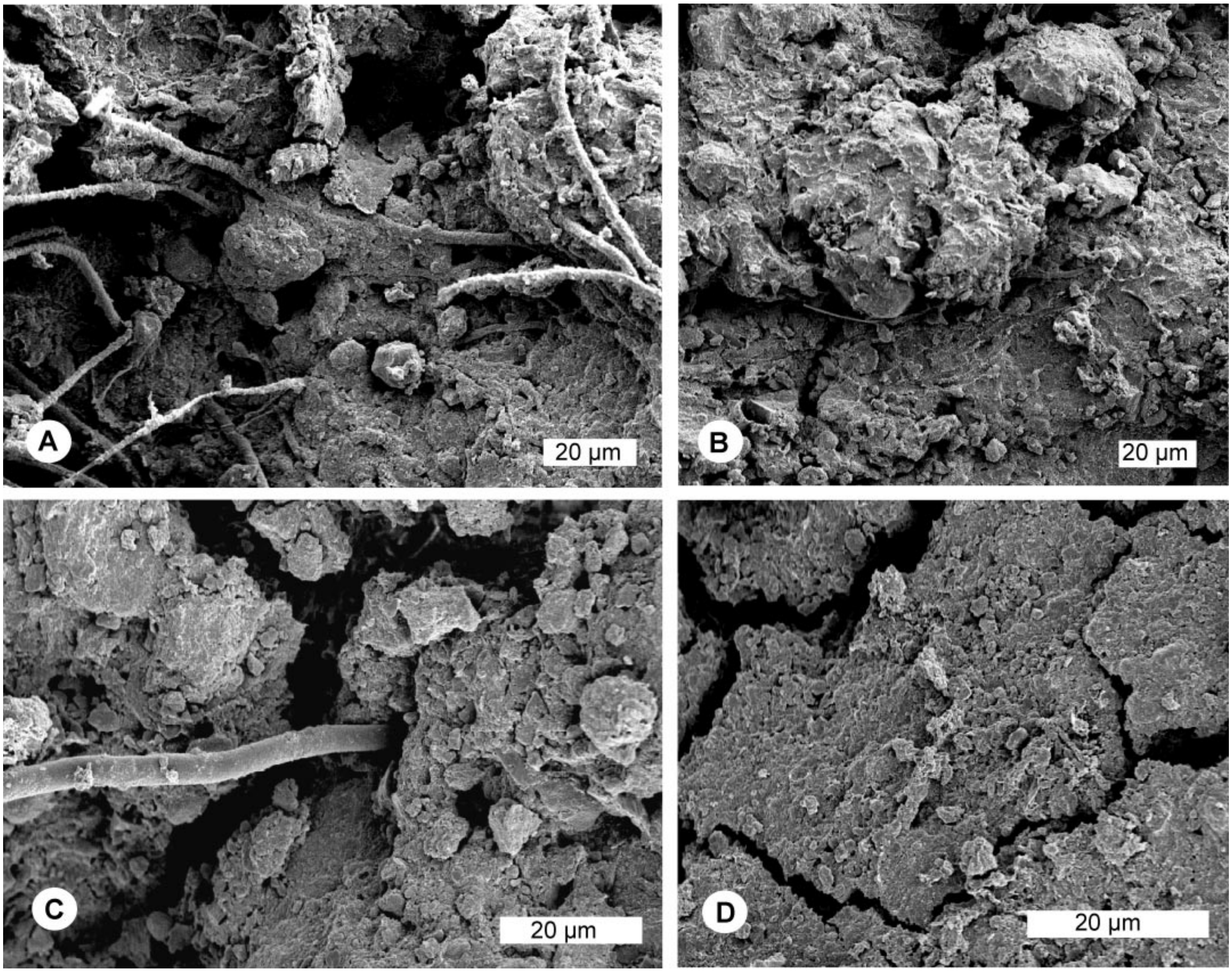

FIG. 10.—SEM microphotographs of clasts in modern pedoliths from the Oregon Cascades and Coast Range: **A, B)** fungal hyphae and fungally imprinted clay films from London; **C, D)** fungally imprinted clay films and decayed fungal remnants from Austa. Scale bars all 20 μm.

seepage leads to rapid crusting, which reduces clayey suspended outwash (Tanaka et al. 1999; Ramos et al. 2003). Individual rare storms can account for as much as 80% of the cumulative 30-year sediment yield from clear-cut forests (Grant and Wolff 1991), and set off numerous debris flows in hilly terrain (Swanston and Swanson 1976). Fires also destroy ground cover, so that large numbers of soil peds roll down hill by dry ravel (Gabet 2003). The transition from clayey soils to silty and sandy sediments is thus a complex process that varies considerably in rate from soil to soil. Many processes conspire to make sepic clasts rare in sedimentary sequences.

PEDOLOGICAL TERMINOLOGY FOR CLAYSTONE BRECCIAS

The bewildering array of soil modifications documented here in earliest Triassic and modern claystone breccias are best described using terminology borrowed from soil science (Brewer 1976; Catt 1990; Retallack 1997a, 2001; Soil Survey Staff 1999). All of the claystone breccias described here are pedoliths, a term used in soil science for redeposited soil (Retallack 2001), and equivalent to the term ''soil sediment'' (Catt 1990). ''Soil sediment'' is confusing because most sediment is derived from the physical erosion of soils, and because sedimentary processes play a role in soil formation (cumulic horizons of Soil Survey Staff 1999). The term pedolith was coined by Erhart (1965) for redeposited laterites, such as those of Vogelsburg and Graulehm in southwest Germany and Lembron in France, which are near their parent lateritic paleosols. In contrast, most sediments have grains so abraded and comminuted that original soil fabrics are no longer visible, nor easily traceable to a particular soil source

A compositional classification of pedoliths can be based on the nature of the most common clasts, borrowing terminology from soil science (Fig. 12). The pedolith used originally to define the term by Erhart (1965) can be called an oxic pedolith, which has opaque ferruginized clasts derived largely from Oxisols, laterites, and bauxites. Such soils and pedoliths are most common in tropical rain forest climates (Bestland et al. 1996), and commonly include abundant, opaque, oxidized, spherical micropeds (Stoops 1983; Retallack 1991). Spherical micropeds of oxic pedoliths are largely produced as oral and fecal pellets of termites (Mermut et al. 1984). Modern pedoliths from Cooper Creek, South Australia (Rust and Nanson 1989; Talbot et al. 1994) are rich in similar kaolinitic ellipsoidal grains like those of nearby deeply weathered tropical soils (Kandosols of R.F. Isbell et al. 1997). Although Rust and Nanson (1989) thought that the clay pellets were eroded from Vertisols, they do not show sepic or argillan

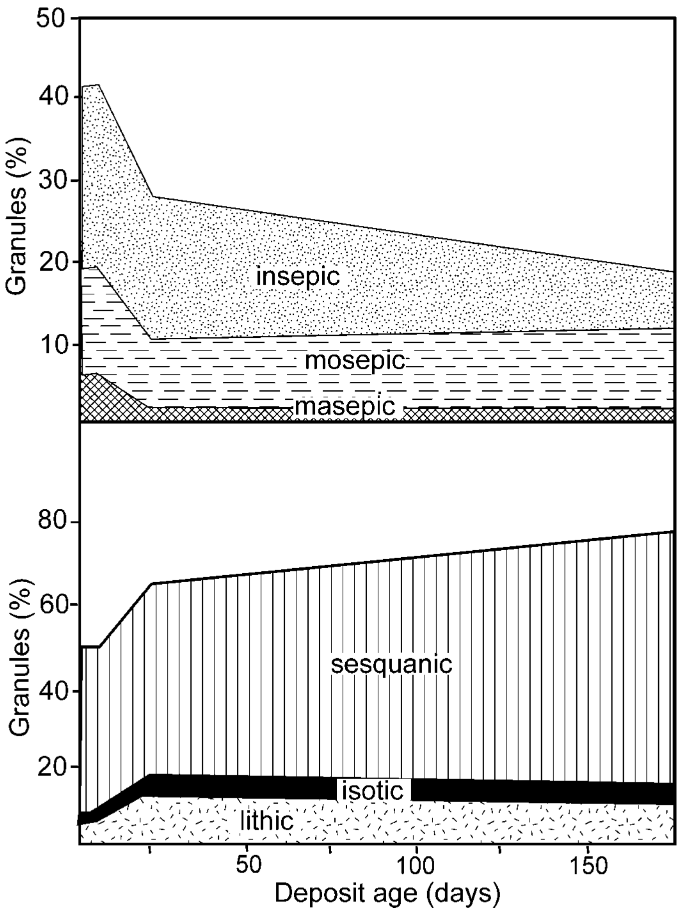

FIG. 11.—Changing proportions of pedogenic clasts through time of a pedolithic debris flow near London, Oregon. Sepic claystone clasts decline dramatically in abundance after only three weeks, but fresh rock fragments (lithic), iron–manganese nodules (isotic), and rock fragments with thick weathering rinds (sesquanic) increase in abundance.

microfabrics of Vertisols (Retallack 1997b) and survive several cycles of transport in flumes (Loch et al. 1991). These are best termed kandic pedoliths, in which clasts are strongly depleted in alkalies and alkaline earths, but little ferruginized. Comparable Triassic kandic pedoliths are described by Talbot et al. (1994) and Müller et al. (2004). Oxic and kandic pedoliths are the most common and widespread kind of pedolith because of their non-slaking grains, but they were not found at the high paleolatitude sites reported here.

The latest Permian claystone breccia from Letham Burn, New Zealand (Fig. 5I) can be termed a sesquanic pedolith, following the term of Brewer (1976) for a thick oxidized weathering rind. These indicate weathering in a humid climate and well drained soil, such as Alfisols and Inceptisols paleosols of the Old Wairaki Hut Formation of Letham Burn (Waterhouse 1998). Such oxidation rinds are common in breccias and conglomerates (Lipple 1984; Retallack 1991), but widely overlooked.

The most widespread kind of Permian–Triassic pedolith in Antarctica (Mt Crean and Coalsack Bluff; Fig. 5F) and Australia (Coalcliff) are full of coal chips and can be called a histic pedolith. This term is derived from the soil-science term histic epipedon for the peaty surface of Histosols of humid areas and waterlogged regions (Soil Survey Staff 1999). Histic pedoliths reported here all overlie fossil Histosols (Retallack 1999a; Retallack and Krull 1999). Histic pedoliths are found in other coal measures as well (Dorsey and Kopp 1985; Nelson et al. 1985), because coal and wood chips are moderately stable in water.

Permian–Triassic boundary pedoliths of the Karoo Basin include abundant redeposited caliche nodules, with diagnostic replacive-micritic and displacive-sparry internal fabrics, like nodules within underlying fossil Aridisols (Lootsberg, Wapadsberg, and Bethulie of Retallack et al. 2003). These can be termed calcic pedoliths, which are widespread because lithified caliche nodules are stable in water (Tandon and Narayan 1981; Retallack 1991; Balin 2002). Only a few Karoo Basin clasts included pseudomorphs of gypsum (Fig. 5G). Silicified pseudomorphs of soil crystals also are common in desert and sabkha soils, and can dominate associated sediments (Southgate et al. 1989; Martini 1994) to form crystic pedoliths. Cold dry deserts with frozen ground can also yield breccias by cryoturbation, slumping, or channel cutting (Young and Long 1976; Brodzikowski and van Loon 1985). Such distinctive deposits of redeposited frigid soil (Gelisols of Soil Survey Staff 1999) can be called a gelic pedolith. Neither crystic nor gelic pedoliths were found in this study, and their rarity reflects the extremity of their climates.

The most intriguing and rare kind of pedolith reported here from Antarctica (Fig. 5C, D; Graphite Peak, Allan Hills) and Australia (Fig. 5H; Wybung Head, Frazer Park) includes mainly clasts with irregular, highly birefringent streaks characteristic of soil aggregates (peds) from subsurface clayey (Bt) horizons of well drained soils (such as non-aquic Vertisols, Alfisols, Ultisols of Soil Survey Staff 1999). This distinctive fabric viewed under crossed nicols in thin section has been called sepic plasmic fabric (by Brewer 1976) and birefringence fabric (by Bullock et al. 1984). A sedimentary deposit with such clasts can be called a sepic pedolith. The ready slaking of comparable soil clasts in clear-cuts of the Oregon Coast Range documented here explains why sepic pedoliths are rare and remarkable.

ALTERNATIVE EXPLANATIONS FOR EARLIEST TRIASSIC CLAYSTONE BRECCIAS

Earliest Triassic breccias and conglomerates have commonly been considered a lag deposit at the base of paleochannels along a major geological disconformity (Collinson et al. 1994; J.L. Isbell and Cuneo 1996). Disconformity lag deposits consist of the most chemically resistant minerals available, such as quartz, chert, and siderite nodules, which are abundant in the bases of paleochannels in the basal Coal Cliff Sandstone and Dooralong Shale of Australia, the Feather Conglomerate and the Fremouw Formation of Antarctica, and the Katberg Formation of South Africa. In contrast, claystone breccias described here contain abundant fragments of soil, including clayey soil aggregates and peat fragments, which are neither structurally nor chemically stable in well aerated water. Furthermore, the conglomerates and breccias known to be of earliest Triassic age are not at the base of sandstone paleochannels, nor do they have a sandy matrix, but are within clayey sequences of paleosols (Retallack 1999a; Retallack and Krull 1999; Retallack et al. 2003).

Shale breccias are also common in the bases of Triassic and Permian fluvial paleochannels in Antarctica (Collinson et al. 1994; J.L. Isbell and Cuneo 1996), Australia (Jones and Rust 1983), South Africa (Retallack et al. 2003), and elsewhere (Plint 1986). They form by rip-up and collapse of banks of recently deposited clayey sediment and very weakly developed, clayey soils. Such shale breccias have sandy matrix to angular, very poorly sorted, clasts of shale, at or near the bases of sandstone paleochannels some 2 to 15 m thick. In contrast, claystone breccias described here are sand-poor, within largely clayey or coaly sequences, and commonly less than 15 cm thick. Furthermore, claystone breccias contain very delicate clasts, such as clayey soil aggregates and peat chips, which do not long endure traction shear or water immersion of fluvial transport.

Another explanation for earliest Triassic breccias and conglomerates is as impact ejecta. This origin is made plausible by the discovery of shocked quartz in the boundary breccias described from Graphite Peak, Mt Crean, and Wybung Head (Retallack et al. 1998), although the Graphite Peak

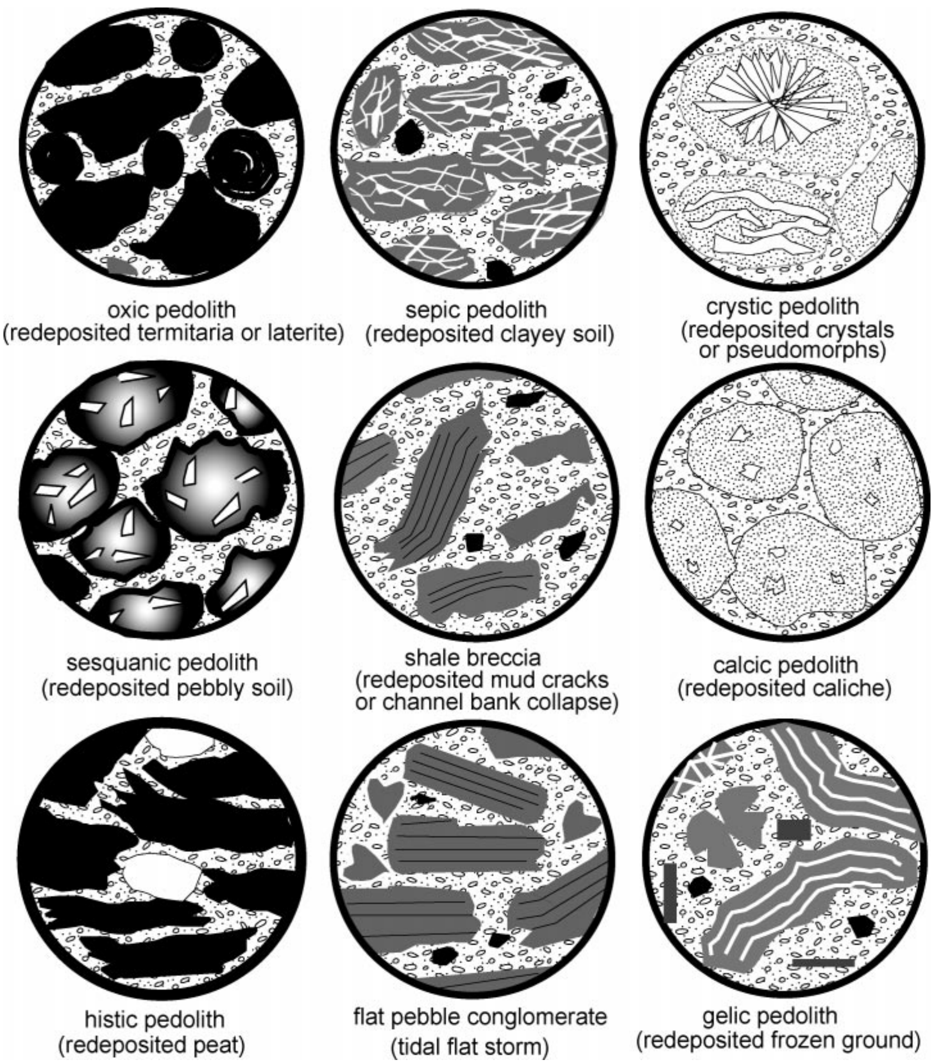

FIG. 12.—Terminology for sepic pedoliths and other comparable coarse grained sediments.

quartz grains are no longer considered shocked (Langenhorst et al. 2005). Shocked quartz has also been reported in claystone breccia at Frazer Park, Australia (Becker et al. 2004), and in other Permian–Triassic boundary beds in India (Shukla et al. 2003), and China (Zhou and Chai 1997). Also found in claystone breccia at Graphite Peak were fragments of meteoritic material and spherules (Basu et al. 2003) and fullerenes with extraterrestrial ^{3}He (Poreda and Becker 2003). A slight, but not replicable iridium anomaly was found in the claystone breccia at Mt Crean, but a comparable anomaly was well below both the claystone breccia and underlying coal at Graphite Peak and Wybung Head (Retallack et al. 1998). However, none of the claystone breccias described here have fused rock or soil like genuine impact breccias (Witzke and Anderson 1996; Koeberl et al. 1996). Furthermore, impact breccias and fallout deposits tend to be even in thickness, and compositionally uniform over large areas, being dominated by material excavated from the impact crater (Fastovsky et al. 1989; Witzke and Anderson 1996; Retallack 2004). In contrast, claystone breccias described here have small amounts of impact-generated debris within a large amount of locally eroded soil material.

Yet another explanation of Permian–Triassic boundary breccias could be as volcanic breccias. At Graphite Peak in Antarctica and Letham Burn in New Zealand the dominant clasts are volcanic rock fragments. Bipyramidal quartz has been found in the claystone breccia at Graphite Peak (Retallack et al. 1998). However, none of the Permian–Triassic claystone breccias show features of volcanic breccias such as vesiculation, fragments of juvenile melt, or zeolites such as natrolite (Laznicka 1988). Furthermore there are few tuffs or other pyroclastic rocks in the Antarctic, Australian, and South African sections, which accumulated hundreds of kilometers north of a volcanic arc (Fig. 1).

Deposition as tempestites by storm waves in tidal flats and estuaries is plausible for sesquanic pedoliths of the Wairaki Breccia of New Zealand (Waterhouse 1998), the flat-pebble conglomerates of Greenland and Austria (Wignall and Twitchett 1999), and well known flat-pebble conglomerates of the Cambrian (Sepkoski 1982). These are massive and crudely bedded deposits of clasts indurated by early cementation and weathering rinds, then cemented by sparry calcite along with marine fossils. Flat-pebble conglomerate clasts have internal lamination not seen in any case discussed here, and some are so rich in organic matter that clasts float in water owing to tiny air bubbles trapped in their microbial mats (Fagerstrom 1967). The winnowing action of successive storm surges explain the paucity of silty and clayey matrix in some flat-pebble conglomerates (Wignall and Twitchett 1999) and the Letham Burn breccias (Waterhouse 1998), unlike all the other cases discussed.

Easily slaked soil clasts can roll downhill dry, as is common in talus cones at the base of hilly topography after forest fires (Gabet 2003; Wondzell and King 2003). This is unlikely for earliest Triassic claystone breccias described here because they lack charcoal and they formed in low-lying sedimentary basins without substantial topographic relief (Collinson et al. 1994). Extremely arid and frigid environments also have colluvial fans of clasts deposited dry or frozen (Brodzikowski and van Loon 1985; Dilliard et al. 1999). In contrast, Permian–Triassic claystone breccias of Antarctica and Australia formed in humid swamplands with only discontinuous permafrost (Retallack 1999a; Retallack and Krull 1999), and those of South Africa do not have abundant crystic clasts of the driest kinds of deserts (Retallack et al. 2003).

For earliest Triassic sepic pedoliths described here, origin in debris flows and mudflows is most likely. A likely mudflow 9 m thick, with matrix-supported clasts of basement rocks up to 7 cm in diameter, has been found at the Permian–Triassic boundary near Banspetali, India (Sarkar et al. 2003). The examples described here, in contrast, are clayey and thin (less than 20 cm and typically 5–12 cm thick). They do have coarse-grained, basal scours and levees marginal to the basal scours, and their profiles are concave over the scour axis (Fig. 3). These are features of thin debris flows, derived from nearby badlands of eroded soils in the Oregon Coast Range and Cascade foothills (Fig. 7).

SEDIMENTARY MODEL FOR EARLIEST TRIASSIC SOIL EROSION

Within the context of modern debris-flow pedoliths associated with road building and clear-cut forestry in the hills of Oregon, where sepic claystone clasts are slaked by a single heavy rainfall, the Permian–Triassic sepic pedoliths of cool temperate, humid regions of the Gondwana supercontinent record an unusually voluminous and short-lived episode of soil erosion. The rarity of sepic pedoliths in sedimentary rocks is not surprising, considering their physical fragility and chemical instability. They call for extraordinary circumstances.

The Permian–Triassic boundary was a rare event of global extent—the greatest mass extinction in the history of life (Jin et al. 2000). Extinctions on land were particularly devastating for lowland plants, such as glossopterids, tree lycopsids, and ruflorian cordaites, whereas upland conifers and seed ferns survived (Retallack 1995; Wang 1996). There was no peat-forming flora for the entire Early Triassic (Retallack et al. 1996), a period of some six million years (Gradstein et al. 2004). Palynological and paleobotanical studies reveal a terminal-Permian dieback of trees, followed by a proliferation of herbaceous horsetails and lycopsids (Retallack 1997b; Looy et al. 2001). Episodes of profound plant decay are indicated by dramatic increases in abundance of spores and hyphae of fungi (Visscher et al. 1996; Steiner et al. 2003), although some of these macerated microfossils are more likely remains of zygnematalean algae from oligotrophic lakes (Krassilov et al. 1999). The cause of such widespread deforestation, decay, and ponding may have been soil anoxia, because berthierine and siderite nodules in earliest Triassic paleosols indicate unusually low soil oxygen (Sheldon and Retallack 2002). There is also carbon isotope evidence for methane pollution of the atmosphere from continental-shelf and permafrost clathrate reservoirs (Krull and Retallack 2000; Krull et al. 2000; Krull et al. 2004). Methane emissions combined with oxidation of biomass and volcanic emissions has been modeled to have reduced atmospheric oxygen to only 12%, well below the current 21% and Permian estimates of 35% (Berner 2002). Such atmospheric and soil anoxia would have been especially difficult for wetland vegetation, whose roots are already challenged for oxygen by stagnant groundwater (Jenik 1976).

Loss of forest cover in lowlands would have created conditions comparable to commercial clear-cutting in Oregon (Fig. 8), with dead stumps and logs littering those parts of the landscape not remodeled by debris-laden water-lines, rills, mudflows, and badlands. The various claystone breccias taken here as evidence of catastrophic soil erosion were overlain, and locally eroded, by the spread of braided streams, distinct from meandering streams of the latest Permian (Retallack 1999a; Retallack and Krull 1999; Ward et al. 2000; Benton 2003).

Within this overall scenario, earliest Triassic claystone breccias are envisaged as local small debris flows from a retreating scarp of erosional badlands in deforested clayey lowland soils (Fig. 13). This wave of erosional gullies eventually sapped sandy soils of higher ground, which then fed widespread alluvial fans and braided streams. The Permian–Triassic life crisis on land thus induced a global soil-erosion crisis broadly comparable to that currently induced by human land clearance.

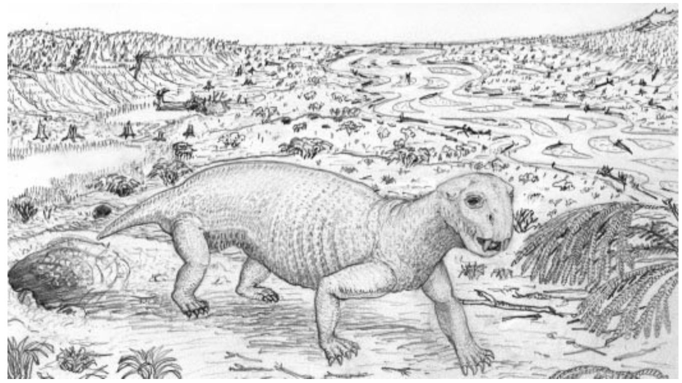

FIG. 13.—Reconstructed earliest Triassic, lowland forest dieback and retreating clayey badlands at Coalcliff, Australia. Plants illustrated include the quillwort *Isoetes beestonii* (Retallack 1997a), and seed fern *Lepidopteris callipteroides* (Retallack 2002b), with upland forests in the background mainly conifers, *Voltziopsis wolganensis* and *V. africanus* (Retallack 1995). The hungry therapsid is *Lystrosaurus curvatus*, known from bones in Antarctica (Colbert 1974) and South Africa (Retallack et al. 2003), but represented only by footprints in the southern Sydney Basin (Retallack 1996).

OTHER SEPIC PEDOLITHS AND SOIL EROSION CRISES

Other crises of soil erosion in the geological past may also be revealed by sepic pedoliths (Table 5). Most of these, such as the Triassic–Jurassic boundary, were also times of global mass extinction (Sepkoski 1986), and postapocalyptic greenhouses revealed by evidence of stomatal indices of fossil plants, and paleosols (Retallack 2002a). I have not yet found sepic pedoliths at any Cretaceous–Tertiary boundary section. Some Cretaceous–Tertiary boundary sections include impact debris, which is only one of a number of differences between the Cretaceous–Tertiary and other extinctions (Retallack 2004). Other sepic pedoliths are evidence that the Permian–Triassic extinction was not the only time of soil erosion crisis.

In the broad sweep of geological history, sepic pedoliths are rare and their antiquity is uncertain. I have seen few histic pedoliths, and they are not widely reported (Dorsey and Kopp 1985; Nelson et al. 1985). Histic pedoliths are unlikely to predate the Devonian origin of peats (Retallack 2001). Other kinds of pedoliths with more durable pedogenic clasts are of greater antiquity: 2.6 Ga for crystic pedoliths (Martini 1994), 2.5 Ga for gelic pedoliths (Young and Long 1976), 2.1 Ga for oxic pedoliths (Gutzmer and Beukes 1998), 1.9 Ga for calcic pedoliths (Campbell and Cecile 1981), and 1.4 Ga for sesquanic pedoliths (Lipple 1984). Many Precambrian paleosols are not sufficiently clayey or pedal to be a source of sepic clasts in overlying alluvium and colluvium (Retallack and Mindszenty 1994; Dilliard et al. 1999). Precambrian Vertisols as ancient as 2.1 Ga have sepic plasmic fabric, but are overlain by fluvial sands containing only scattered non-sepic iron-manganese-stained soil peds from paleosol surface horizons (Retallack 1986, 1997a; Retallack and Krinsley 1993). Thus there is potential for Precambrian sepic pedoliths, but the spread of clayey forested soils since the Devonian (Retallack 2001) may explain why only Phanerozoic examples are known so far (Table 5).

CONCLUSIONS

Earliest Triassic and modern claystone breccias described here are distinctive because their clasts show modifications due to soil formation. The

TABLE 5.—*Other sepic pedioliths worthy of further investigation.*

Age (Ma)	Period/Epoch	Stage	Formation	Location	Coordinates	Reference
35	late Eocene	Chadronian	Chadron Formation	Badlands National Park, South Dakota	W102.22500° N43.850556°	Retallack 1983
94	Cretaceous	Cenomanian	Dakota Formation	south of Hoisington, Kansas	W98.78722° N38.467778°	Retallack and Dilcher 1981
117	earliest Cretaceous	Aptian	Yellow Cat Mbr, Cedar Mountain Fm	north of Moab, Utah	W109.69187° N39.71892°	Kirkland et al. 1999
200	earliest Jurassic	Hettangian	Shuttle Meadow Formation	south of Northampton, Massachusetts	W72.651389° N42.29861°	Gierlowski-Kordesch 1998
217	late Triassic	late Carnian	Lockatong Formation	Hudson River, Palisades State Park, New York	W73.90500° N41.009722°	Van Houten 1969; Sanders 1972
245	latest Early Triassic	Spathian	Grès a Meule	near Hangviller, France	E7.23333° N48.81667°	Gall and Grauvogel-Stamm 1999
245	latest Early Triassic	Spathian	Garie Formation	Turimetta Head, Australia	W151.31750° S33.706944°	Retallack 1976
260	mid-Permian	Capitanian-Kazanian	Flowerpot Formation	southwest of Loyal, Oklahoma	W98.152744° N35.914583°	Olson and Barghusen 1962
270	early-mid Permian	Kungurian–Leonardian	Hennessy Formation	east of Manitou, Oklahoma	W98.902292° N34.509306°	Olson 1967
270	early–mid Permian	Kungarian–Leonardian	Hennessy Formation	in Purcell, Oklahoma	W97.360611° N35.024389°	Olson 1967
299	earliest Permian	Asselian–Wolfcampian	Wellington Formation	southeast of Paoli, Oklahoma	W97.246139° N35.808639°	Olson 1967

array of soil-derived clasts in these claystone breccias is matched by paleosols or soils at the same locality. Although earliest Triassic and modern soil erosion have been widespread, sources were local. Some kinds of soil clasts are robust and common, such as caliche and ferruginous nodules. Delicate clayey soil aggregates (peds) with soil microfabric (sepic plasmic fabric) are rarely encountered in sediments, because they dissolve in water. However, sepic clasts are locally common in redeposited soils (pedoliths) formed at the Permian–Triassic boundary and in mudflows of Oregon forest clearcuts. Such sepic pedoliths indicate major soil-erosion crises during extraordinary circumstances, such as human forest clear-cutting and forest die-back due to terminal-Permian atmospheric pollution with methane and other noxious gases. Other episodes of severe soil erosion may be represented by comparable deposits at the Triassic–Jurassic boundary and other times of life crisis.

ACKNOWLEDGMENTS

Carolyn Phillips helped during laboratory and field work in Oregon and Antarctica. Many very difficult thin sections were prepared by Alicia Duncan. Antarctic field work was aided by Shaun Norman, Roger Smith, Nathan Sheldon, Ramananda Chakrabarti, Evelyn Krull, Christine Metzger, Scott Robinson, and Luann Becker. South African fieldwork was done with Peter Ward, Roger Smith, and Roger Buick. David Hofflein of Roseburg Resources, Pamela White of Weyerhauser Corporation, and Alan Corbin of Eugene Bureau of Land Management helped with logging information. Funded by National Science Foundation grant OPP0230086.

REFERENCES

AMEZKETA, E., SINGER, M.J., AND LE BISSONAIS, Y., 1996, Testing a new procedure for measuring water stable aggregates: Soil Science Society of America, Journal, v. 60, p. 888–894.
ANDERSON, J.M., AND ANDERSON, H.M., 1985, Palaeoflora of Southern Africa: Prodromus of South African Megafloras: Devonian to Lower Cretaceous: Rotterdam, A.A. Balkema, 423 p.
BAJRACHARYA, R.M., AND LAL, R., 1998, Crusting processes under simulated rainfall on a tropical Alfisol: Hydrological Processes, v. 12, p. 1927–1938.
BALIN, D.F., 2002, Calcrete morphology and karst development in the upper Old Red Sandstone at Milton Ness, Scotland, *in* Friend, P.F., and Williams, B.P.J., eds., New Perspectives on the Old Red Sandstone: Geological Society of London, Special Publication, v. 180, p. 485–501.
BARTHES, B., AND ROOSE, E., 2002, Aggregate stability as an indicator of soil susceptibility to runoff and erosion: validation at several levels: Catena, v. 47, p. 133–149.
BASU, A.R., PETAEV, M.I., POREDA, R.J., JACOBSEN, S.B., AND BECKER, L., 2003, Chondritic meteorite fragments associated with the Permian–Triassic boundary in Antarctica: Science, v. 302, p. 1388–1392.
BAUD, A., MAGARITZ, M., AND HOLSER, W.T., 1989, Permian–Triassic of the Tethys: carbon isotope studies: Geologische Rundschau, v. 78, p. 649–677.
BECKER, L., POREDA, R.J., BASU, A.R., POPE, K.O., HARRISON, T.M., NICHOLSON, C., AND IASKY, R., 2004, Bedout: a possible end-Permian impact crater offshore of northwestern Australia: Science, v. 304, p. 1469–1476.
BENTON, M.J., 2003, When Life Nearly Died: New York, Thames and Hudson, 336 p.
BERNER, R.A., 2002, Examination of hypotheses for the Permian–Triassic boundary extinction by carbon cycle modeling: U.S. National Academy of Sciences, Proceedings, v. 99, p. 4172–4177.
BESTLAND, E.A, RETALLACK, G.J., RICE, A.E., AND MINDSZENTY, A., 1996, Late Eocene detrital laterites in central Oregon: mass balance geochemistry, depositional setting and landscape evolution: Geological Society of America, Bulletin, v. 108, p. 285–302.
BREWER, R., 1976, Fabric and Mineral Analysis of Soils: New York, Krieger, 482 p.
BRODZIKOWSKI, K., AND VAN LOON, A.J., 1985, Penecontemporaneous non-tectonic brecciation of unconsolidated silts and muds: Sedimentary Geology, v. 41, p. 269–282.
BULLOCK, P., FÉDEROFF, N., JONGERIUS, A., STOOPS, G., AND TURSINA, T., 1984, Handbook of Soil Thin Section Description: Albrighton, U.K., Waite Research, 154 p.
CAMPBELL, F.H.A., AND CECILE, M.P., 1981, Evolution of the early Proterozoic Kilohigok Basin, Bathurst Inlet–Victoria Island, Northwest Territories, *in* Campbell, F.H.A., ed., Proterozoic Basins of Canada: Geological Survey of Canada, Paper, v. 81–10, p. 103–137.
CATT, J.A., 1990, Paleopedology manual: Quaternary International, v. 6, p. 1–95.
COLBERT, E.H., 1974, *Lystrosaurus* from Antarctica: American Museum Novitates, v. 2535, p. 1–44.
COLLINSON, J.W., ISBELL, J.I., ELLIOT, J.H., MILLER, M.F., MILLER, J.M.G., AND VEEVERS, J.J., 1994, Permian–Triassic Transantarctic Basin, *in* Veevers, J.J., and Powell, C.M.A., eds., Permian–Triassic Pangean Basins and Foldbelts along the Panthalassan Margin of Gondwanaland: Geological Society of America, Memoir 184, p. 173–222.
D'AQUI, L.P., CHURCHMAN, G.J., JANIK, L.J., RISTORI, G.G., AND WEISSMAN, D.A., 1999, Effect of organic matter removal by low temperature ashing on dispersion of undisturbed aggregates from a tropical crusting soil: Geoderma, v. 93, p. 311–324.
DAVIES, G.R., MOSLOW, T.F., AND SHERWIN, M.D., 1997, The lower Triassic Montney Formation, west central Alberta: Bulletin of Canadian Petroleum Geologists, v. 45, p. 474–505.
DE WIT, M.J., GHOSH, J.G., DE VILLIERS, S., RAKOTOSOLOFO, N., ALEXANDER, J., TRIPATHI, A., AND LOOY, C., 2002, Multiple organic carbon isotope reversals across the Permo-Triassic boundary of terrestrial Gondwanan sequences: clues to extinction patterns and delayed ecosystem recovery: Journal of Geology, v. 110, p. 227–240.
DIESSEL, C.F.K., 1992, Coal-bearing Depositional Systems: Berlin, Springer, 721 p.
DILLIARD, K.A., SIMPSON, E.L., AND NOTO, R.C., 1999, A Neoproterozoic paleosurface and associated colluvial and fluvial deposits, Shenandoah National Park, Virginia: Southeastern Geology, v. 38, p. 239–257.
DORSEY, A.E., AND KOPP, O.C., 1985, Distribution of elements and minerals between a coal and its overlying sedimentary rocks in a limnic environment: International Journal of Coal Geology, v. 5, p. 261–274.
EKANAYAKE, J.C., MARDEN, M., WATSON, A.J., AND ROWAN, D., 1997, Tree roots and slope stability: a comparison between *Pinus radiata* and kãnuka: New Zealand Journal of Forestry Science, v. 27, p. 216–223.
ENGELEN, G.B., 1973, Runoff processes and slope development in Badlands National Monument, South Dakota: Journal of Hydrology, v. 18, p. 55–79.
ERHART, H., 1965, Le temoinage paléoclimatique de quelques formations paléopediques dans leur rapport avec la sedimentologie: Geologische Rundschau, v. 54, p. 15–23.
FAGERSTROM, J.A., 1967, Development, flotation and transportation of mud crusts: neglected factors in sedimentology: Journal of Sedimentary Petrology, v. 37, p. 73–79.
FARABEE, M.J., TAYLOR, E.L., AND TAYLOR, T.N., 1991, Late Permian palynomorphs from the Buckley Formation, central Transantarctic Mountains, Antarctica: Review of Palaeobotany and Palynology, v. 69, p. 353–368.
FASTOVSKY, D.E., MCSWEENEY, K., AND NORTON, L.D., 1989, Pedogenic development at the

Cretaceous–Tertiary boundary, Garfield County, Montana: Journal of Sedimentary Petrology, v. 59, p. 758–767.
FAULKNER, H., ALEXANDER, R., AND WILSON, B.R., 2003, Changes to dispersive characteristics of soils along an evolutionary slope in Spain: implications for site stabilization: Catena, v. 50, p. 243–254.
FLÜGEL, E., 1994, Pangean shelf carbonates: controls and paleoclimatic significance of Permian and Triassic reefs, *in* Klein, G.deV., ed., Pangea: paleoclimate, tectonics and sedimentation during accretion, zenith and breakup of a supercontinent: Geological Society of America, Special Paper, v. 288, p. 247–266.
FORCE, L.M., 1975, Stratigraphy and paleoecology of the Productus Creek Group, South Island, New Zealand: New Zealand Journal of Geology and Geophysics, v. 18, p. 373–398.
GABET, E.J., 2003, Sediment transported by dry ravel: Journal of Geophysical Research, v. 108, n. 1, 8 p. (DOI: 10.1029/20DIJB001686).
GALL, J.-C., AND GRAUVOGEL-STAMM, L., 1999, Paläoökologie des oberen Buntsandsteins am Westrand des Germanischen Beckens: Der Voltziensandstein im nordöstlichen Frankreich als deltaische Bildung, *in* Hauschke, N. and Wilde, V., eds., Trias: eine Ganz andere Welt: München, Friedrich Pfeil, p. 283–298.
GIERLOWSKI-KORDESCH, E.H., 1998, Carbonate deposition in an ephemeral siliciclastic alluvial system: Jurassic Shuttle Meadow Formation, Newark Supergroup, Hartford basin, U.S.A.: Palaeogeography, Palaeoclimatology, Palaeoecology, v. 140, p. 161–184.
GRADSTEIN, F.M., OGG, J.G., AND SMITH, A.G., 2004, A Geological Time Scale 2004: Cambridge, U.K., Cambridge University Press (in press).
GRANT, G.E., AND WOLFF, A.L., 1991, Long term patterns of sediment transport after timber harvest, western Cascade Mountains, Oregon, USA, *in* Peters, N.E., and Walling, D.E., eds., Sediment and Stream Water Quality in a Changing Environment: Trends and Explanation: International Association of Hydrological Science, Publication 203, p. 31–40.
GUTZMER, J., AND BEUKES, N.J., 1998, Earliest laterites and possible evidence for vegetation in the early Proterozoic: Geology, v. 26, p. 430–441.
ISBELL, J.L., AND CUNEO, N.R., 1996, Depositional framework of Permian coal-bearing strata, southern Victoria Land, Antarctica: Palaeogeography, Palaeoclimatology, Palaeoecology, v. 125, p. 217–238.
ISBELL, J.L., ASKIN, R.A., AND RETALLACK, G.J., 1999, Search for evidence of impact at the Permian–Triassic boundary in Antarctica and Australia: comment and reply: Geology, v. 27, p. 859–860.
ISBELL, R.F., MCDONALD, W.J., AND ASHTON, L.J., 1997, Concepts and Rationale of the Australian Soil Classification: Canberra, Australia, Commonwealth Science and Industrial Research Organization, Land and Water, 152 p.
JENIK, J., 1976, Roots and root systems in tropical trees: morphologic and ecologic aspects, *in* Tomlinson, P.B., and Zimmerman, M.H., eds., Tropical Trees as Living Systems: Cambridge, U.K., Cambridge University Press, p. 323–349.
JIN, Y.-G., WANG, Y., WANG, W., SHANG, Q.H., CAO, C.Q., AND ERWIN, D.H., 2000, Pattern of marine mass extinction near the Permian–Triassic boundary in South China: Science, v. 289, p. 432–436.
JONES, B.G., AND RUST, B.R., 1983, Massive sandstone facies in the Hawkesbury Sandstone, a Triassic fluvial deposit near Sydney, Australia: Journal of Sedimentary Petrology, v. 53, p. 1249–1259.
KIRKLAND, J.I., CIFELLI, R.L., BRITT, B.B., BURGE, P.L., DE COURTEN, F.L., EATON, J.G., AND PARRISH, J.M., 1999, Distribution of vertebrate faunas in the Cedar Mountain Formation, east central Utah, *in* Gillette, D.D., ed., Vertebrate Paleontology in Utah: Utah Geological Survey, Miscellaneous Publication 99–1, p. 201–217.
KNOLL, A.H., BAMBACH, R.K., CANFIELD, D.E., AND GROTZINGER, J.P., 1996, Comparative Earth history and the Late Permian mass extinction: Science, v. 273, p. 452–457.
KOEBERL, C., REIMOLD, W.U., KRACHER, A., TRÄXLER, B., VORMAIER, A., AND KÖRNER, W., 1996, Mineralogical, petrological, and geochemical studies of drill core samples from the Manson Impact Structure, *in* Koeberl, C., and Anderson, R.R., eds., The Manson Impact Structure, Iowa: Anatomy of an Impact Crater: Geological Society of America, Special Paper, v. 302, p. 145–219.
KOZUR, H.W., 1993, Annotated correlation tables of the Germanic Buntsandstein and Keuper, *in* Lucas, S.G., and Morales, M., eds., The Nonmarine Triassic: New Mexico Museum of Natural History and Science, Bulletin, v. 3, p. 243–248.
KRASSILOV, V.A., AFONIN, S.A., AND BARANOVA, S.S., 1999, *Tympanicysta* and the terminal Permian events: Permophiles, v. 35, p. 16–17.
KRULL, E.S., AND RETALLACK, G.J., 2000, $\delta^{13}C$ profiles from paleosols across the Permian–Triassic boundary: evidence for methane release: Geological Society of America, Bulletin, v. 112, p. 1459–1472.
KRULL, E.S., RETALLACK, G.J., CAMPBELL, H.J., AND LYON, G.L., 2000, $\delta^{13}C_{org}$ chemostratigraphy of the Permian–Triassic boundary in the Maitai Group, New Zealand: evidence for high latitude methane release: New Zealand Journal of Geology and Geophysics, v. 43, p. 21–32.
KRULL, E.S., LEHRMANN, D.J., DRUKE, D., KESSEL, B., YU, Y.-Y., AND LI, R.-X., 2004, Stable carbon isotope stratigraphy across the Permian–Triassic boundary in shallow marine carbonate platforms, Nanpanjiang Basin, South China: Palaeogeography, Palaeoclimatology, Palaeoecology, v. 204, p. 297–315.
LANDIS, C.A., CAMPBELL, H.J., ASLUND, T., CAWOOD, P.A., DOUGLAS, A., KIMBROUGH, D.L., PILLAI, D.D.L., RAINE, J.I., AND WILLSMAN, A., 1999, Permian–Jurassic strata at Productus Creek, Southland, New Zealand: implications for terrane dynamics of the eastern Gondwanaland margin: New Zealand Journal of Geology and Geophysics, v. 42, p. 255–278.
LAZNICKA, P., 1988, Breccias and Coarse Fragmentites: Petrology, Environments, Associations, Ores: Amsterdam, Elsevier, 832 p.
LANGENHORST, F., KYTE, F.T., AND RETALLACK, G.J., 2005, Reexamination of quartz grains from the Permian–Triassic boundary section at Graphite Peak, Antarctica: Lunar and Planetary Science Conference, Abstracts (in press).
LE BISSONAIS, Y., 1996, Aggregate stability and assessment of soil crustability and erodibility: theory and methodology: European Journal of Soil Science, v. 47, p. 425–452.
LEHRMANN, D.J., PAYNE, J.L., FELIX, S.V., DILLETT, P.M., WANG, H.M., YU, Y.-Y., AND WEI, J.Y., 2003, Permian–Triassic boundary sections from shallow-marine carbonate platforms of Nanpanjiang Basin, south China: implications for oceanic conditions associated with the end-Permian extinction and its aftermath: Palaios, v. 18, p. 138–152.
LINDBO, D.L., AND RHOTON, F.E., 1996, Slaking in fragipan and argillic horizons: Soil Science Society of America, Journal, v. 60, p. 552–554.
LIPPLE, S.L., 1984, Proterozoic mass-transported breccias, Nereeno Hill, Western Australia: Geological Survey of Western Australia, Report, v. 12, p. 62–71.
LOCH, R.J., RUST, B.R., AND NANSON, G.L., 1991, Bedload transport of mud as pedogenic aggregates in modern and ancient rivers: discussion and reply: Sedimentology, v. 38, p. 157–160.
LOOY, C.V., TWITCHETT, R.J., DILCHER, D.L., VAN KONIJNENBERG-VAN CITTERT, J.H.A., AND VISSCHER, H., 2001, Life in the end-Permian dead zone: U.S. National Academy of Sciences, Proceedings, v. 98, p. 7879–7883.
MACLEOD, K.G., SMITH, R.M.H., KOCH, P.L., AND WARD, P.D., 2000, Timing of mammal-like reptile extinction across the Permian/Triassic boundary in South Africa: Geology, v. 24, p. 227–230.
MANAENKOV, I.V., ZUNKOVA, T.A., AND KARPACHEVSKII, L.O., 1997, Mechanical resistance of differently shaped peds: Eurasian Soil Science, v. 30, p. 1287–1293.
MARTINI, J.E.J., 1994, A late Archaean–Palaeoproterozoic (2.6 Ga) palaeosol on ultramafics in the eastern Transvaal, South Africa: Precambrian Research, v. 67, p. 159–180.
MARUOKA, T., KOEBERL, C., HANCOX, P.J., AND REIMOLD, W.U., 2003, Sulfur geochemistry across a terrestrial Permian–Triassic boundary section in the Karoo Basin, South Africa: Earth and Planetary Science Letters, v. 206, p. 101–117.
MCMANUS, H.A., TAYLOR, E.L., TAYLOR, T.N., AND COLLINSON, J.W., 2002, A petrified *Glossopteris* flora from Collinson Ridge, central Transantarctic Mountains: Late Permian or Early Triassic?: Review of Palaeobotany and Palynology, v. 120, p. 233–246.
MERMUT, A.R., ARSHAD, M.A., AND ST. ARNAUD, F.J., 1984, Micropedological study of termite mounds of three species of *Macrotermes*: Soil Science Society of America, Journal, v. 48, p. 613–620.
MOORE, D., AND SINGER, M., 1990, Crust formation effect on soil erosion properties: Soil Science Society of America, Journal, v. 54, p. 1117–1123.
MORANTE, R., 1996, Permian and Early Triassic isotopic records of carbon and strontium in Australia and a scenario of events about the Permian–Triassic boundary: Historical Biology, v. 11, p. 289–310.
MÜLLER, R., NYSTNEN, J.P., AND WRIGHT, V.R., 2004, Pedogenic aggregates and paleosol development in ancient dryland river systems: criteria for interpreting mudrock origin and floodplain dynamics: Journal of Sedimentary Research, v. 74, p. 537–551.
NELSON, W.J., EGGERT, D.L., DIMICHELLE, W.A., AND STEYCK, A.C., 1985, Origin of discontinuities in coal-bearing strata at Roaring Creek (basal Pennsylvanian of Indiana): International Journal of Coal Geology, v. 4, p. 355–370.
OLSON, E.C., 1967, Early Permian vertebrates: Oklahoma Geological Survey, Circular 74, 111 p.
OLSON, E.C., AND BARGHUSEN, H.R., 1962, Vertebrates from the Flowerpot Formation, Permian of Oklahoma. Part 1 of Permian Vertebrates from Oklahoma and Texas: Oklahoma Geological Survey, Circular 59, p. 5–48.
PARE, T., DINEL, H., MOULIN, P., AND TOWNLEY-SMITH, L., 1999, Organic matter quality and structural stability of a black chernozemic soil under different manure and tillage practices: Geoderma, v. 91, p. 311–326.
PARSONS, R.B., 1978, Soil–geomorphology relations in mountains of Oregon: Geoderma, v. 21, p. 25–39.
PATCHING, W.R., 1987, Soil Survey of Lane County: Washington, D.C., U.S. Government Printing Office, 369 p.
PETTIJOHN, F.J., 1975, Sedimentary Rocks: New York, Harper & Row, 628 p.
PLINT, A.G., 1986, Slump blocks, intraformational conglomerates and associated erosional structures in Pennsylvanian fluvial strata of Eastern Canada: Sedimentology, v. 33, p. 387–399.
POREDA, R.J., AND BECKER, L., 2003, Fullerenes and interplanetary dust at the Permian–Triassic boundary: Astrobiology, v. 3, p. 75–90.
RAMOS, M.C., NACCI, S., AND PLA, I., 2003, Effect of raindrop impact and its relationship with aggregate stability to different aggregation forces: Catena, v. 53, p. 365–376.
REICHERT, J.M., AND NORTON, L.D., 1994, Aggregate stability and rain-impacted sheet erosion of air-dried and pre-wet clayey surface soils under intense rain: Soil Science, v. 158, p. 159–169.
RETALLACK, G.J., 1976, Triassic palaeosols in the upper Narrabeen Group of New South Wales. Part I: Features of the palaeosols: Geological Society of Australia, Journal, v. 23, p. 383–399.
RETALLACK, G.J., 1983, Late Eocene and Oligocene paleosols in Badlands National Park, South Dakota: Geological Society of America, Special Paper, v. 193, 82 p.
RETALLACK, G.J., 1986, Reappraisal of a 2200-Ma-old paleosol from near Waterval Onder, South Africa: Precambrian Research, v. 32, p. 195–232.
RETALLACK, G.J., 1991, Miocene Paleosols and Ape Habitats in Pakistan and Kenya: New York, Oxford University Press, 346 p.
RETALLACK, G.J., 1995, Permian–Triassic life crisis on land: Science, v. 267, p. 77–80.
RETALLACK, G.J., 1996, Early Triassic therapsid footprints from the Sydney Basin, Australia: Alcheringa, v. 20, p. 301–314.
RETALLACK, G.J., 1997a, A Colour Guide to Paleosols: Chichester, Wiley, 175 p.
RETALLACK, G.J., 1997b, Earliest Triassic origin of *Isoetes* and quillwort evolutionary radiation: Journal of Paleontology, v. 71, p. 500–521.
RETALLACK, G.J., 1999a, Post-apocalyptic greenhouse paleoclimate revealed by earliest Triassic

paleosols in the Sydney Basin, Australia: Geological Society of America, Bulletin, v. 111, p. 52–70.

Retallack, G.J., 1999b, A Jurassic prehnite vein intruding the Permian–Triassic boundary at Graphite Peak, Antarctica: Antarctic Journal of the U.S., v. 30, n. 5, p. 5–7.

Retallack, G.J., 2001, Soils of the Past: Oxford, Blackwell, 404 p.

Retallack, G.J., 2002a, Carbon dioxide and climate over the past 300 Myr: Royal Society (London), Philosophical Transactions, v. A360, p. 659–673.

Retallack, G.J., 2002b, *Lepidopteris callipteroides* (Carpentier) comb. nov., an earliest Triassic seed fern of the Sydney Basin, southeastern Australia: Alcheringa, v. 26, p. 475–500.

Retallack, G.J., 2004, Acid rain as a selective extinction mechanism between birds and dinosaurs, *in* Currie, P., Koppelhus, E., and Wright, J., eds., Feathered Dragons: the Evolutionary Transition between Birds and Dinosaurs: Indanapolis, Indiana University Press, p. 35–64.

Retallack, G.J., and Dilcher, D.L., 1981, Early angiosperm reproduction: *Prisca reynoldsii* gen. et sp. nov., from mid-Cretaceous coastal deposits in Kansas, U.S.A.: Palaeontographica, v. B179, p. 103–137.

Retallack, G.J., and Hammer, W.R., 1998, Paleoenvironment of the Triassic therapsid *Lystrosaurus* in the central Transantarctic Mountains, Antarctica: Antarctic Journal of the U.S., v. 31, n. 5, p. 33–35.

Retallack, G.J., and Krinsley, D.E., 1993, Metamorphic alteration of a Precambrian (2.2 Ga) paleosol from South Africa revealed by back-scatter imaging: Precambrian Research, v. 63, p. 27–41.

Retallack, G.J., and Krull, E.S., 1999, Landscape ecological shift at the Permian–Triassic boundary in Antarctica: Australian Journal of Earth Sciences, v. 46, p. 785–812.

Retallack, G.J., and Mindszenty, A., 1994, Well preserved Late Precambrian paleosols from northwest Scotland: Journal of Sedimentary Research, v. A64, p. 264–281.

Retallack, G.J., Veevers, J.J., and Morante, R., 1996, Global Early Triassic coal gap between Late Permian extinction and Middle Triassic recovery of peat-forming plants: Geological Society of America, Bulletin, v. 108, p. 195–207.

Retallack, G.J., Seyedolali, A., Krull, E.S., Holser, W.T., Ambers, C.A., and Kyte, F.T., 1998, Search for evidence of impact at the Permian–Triassic boundary in Antarctica and Australia: Geology, v. 26, p. 979–982.

Retallack, G.J., Smith, R.M.H., and Ward, P.D., 2003, Vertebrate extinction across the Permian–Triassic boundary in Karoo Basin, South Africa: Geological Society of America, Bulletin, v. 115, p. 1133–1152.

Retallack, G.J., Orr, W.N., Prothero, D.R., Duncan, R.A., Kester, P.R., and Ambers, C.P., 2004, Eocene–Oligocene extinction and paleoclimatic change near Eugene, Oregon: Geological Society of America, Bulletin, v. 116, p. 817–839.

Retallack, G.J., Jahren, H., Sheldon, N.D., Chakrabarti, R., Metzger, C.A., and Smith, R.M.H., 2005, The Permian–Triassic boundary in Antarctica: Antarctic Research (in press).

Rienks, S.M., Botha, G.A., and Hughes, J.C., 2000, Some physical and chemical properties of sediments exposed in a gully (donga) in northern KwaZulu-Natal, South Africa and their relationship to the erodibility of the colluvial layers: Catena, v. 39, p. 11–31.

Rosenfeld, C.L., 2000, Forest engineering amplification of storm-induced mass-wasting in the Oregon Coast Range, USA: Geomorphology, v. 31, p. 217–228.

Rust, B.R., and Nanson, G.C., 1989, Bedload transport of mud as pedogenic aggregates in modern and ancient rivers: Sedimentology, v. 36, p. 291–306.

Sanders, J.E., 1972, Sedimentology and general structure of the northern portion of the Newark Basin: National Association of Geology Teachers, Eastern Section, Field Trip Guidebook, 14 p.

Sarkar, A., Yoshioka, H., Ebihara, M., and Naraoka, H., 2003, Geochemical and organic carbon isotope studies across the continental Permo-Triassic boundary of Raniganj Basin, eastern India: Palaeogeography, Palaeoclimatology, Paleoecology, v. 191, p. 1–14.

Schmidt, K.M., Roering, J.L., Stock, J.D., Dietrich, W.E., Montgomery, D.R., and Schaub, T., 2001, The variability of root cohesion as an influence on shallow landslide susceptibility in the Oregon Coast Range: Canadian Geotechnical Journal, v. 38, p. 995–1024.

Schubert, J.K., and Bottjer, D.J., 1992, Early Triassic stromatolites as post-extinction disaster forms: Geology, v. 20, p. 883–886.

Schumm, S.A., 1962, Erosion of miniature pediments in Badlands National Monument, South Dakota: Geological Society of America, Bulletin, v. 73, p. 719–724.

Scotese, C.R., 2001, Atlas of Earth History, volume 1, Paleogeography: PALEOMAP Project, Arlington, Texas, 52 p. (web page http:/www.scotese.com/newpages.htm)

Sepkoski, J.J., 1982, Flat-pebble conglomerates, storm deposits, and the Cambrian bottom fauna, *in* Einsele, G., and Seilacher, A., eds., Cyclic and Event Stratification: Berlin, Springer, p. 371–385.

Sepkoski, J.J., 1986, Patterns of Phanerozoic extinction: a perspective from global data bases, *in* Walliser, O.H., ed., Global Events and Event Stratigraphy in the Phanerozoic: Berlin, Springer, p. 35–51.

Shainberg, I., Levy, G.J., Levin, J., and Goldstein, D., 1997, Aggregate size and seal properties: Soil Science, v. 162, p. 470–478.

Sheldon, N.D., and Retallack, G.J., 2002, Low oxygen levels in earliest Triassic soils: Geology, v. 30, p. 919–922.

Sheldon, N.D., Retallack, G.J., and Tanaka, S., 2002, Geochemical climofunctions from North American soils and application to paleosols across the Eocene–Oligocene boundary in Oregon: Journal of Geology, v. 110, p. 687–696.

Shukla, A.D., Bhandari, N., and Shukla, P.N., 2003, Shocked quartz at the Permian–Triassic boundary (P/T) in Spiti Valley, Himalaya, India: Lunar and Planetary Science, Abstracts, v. 34, p. 1490.

Smith, R.M.H., and Ward, P.D., 2001, Pattern of vertebrate extinction across an event bed at the Permian–Triassic boundary in the Karoo Basin of South Africa: Geology, v. 29, p. 1147–1150.

Soil Survey Staff, 1999, Keys to Soil Taxonomy: Blacksburg, Virginia, Pocahontas Press, 600 p.

Sood, M.C., and Chaudhary, T.N., 1980, Sod erosion and runoff from a sandy loam soil in relation to initial clod size, tillage-time moisture, and residue mulching under similated rainfall: Journal of Indian Soil Science, v. 28, p. 24–27.

Southgate, P.N., Lambert, I.N., Donelly, T.H., Henry, R., Eetminan, H., and Weste, G., 1989, Depositional environments and diagenesis of Lake Parakellya: a Cambrian alkaline playa from the Officer Basin, South Australia: Sedimentology, v. 36, p. 1091–1112.

Steiner, M.B., Eshet, Y.E., Rampino, M.R., and Schwindt, D.M., 2003, Fungal abundance spike and the Permian–Triassic boundary in the Karoo Supergroup (South Africa): Palaeogeography, Palaeoclimatology, Palaeoecology, v. 194, p. 405–414.

Stoops, G., 1983, Micromorphology of oxic horizons, *in* Bullock, P., and Murphy, C., eds., Soil Micromorphology, vol. 1, Techniques and Applications: Berkhamstead, U.K., Academic Press, p. 419–440.

Swanson, F.J., and Dyrness, C.T., 1975, Impact of clear-cutting and road construction on soil erosion by landslides in the western Cascade Range, Oregon: Geology, v. 3, p. 393–396.

Swanston, D.N., and Swanson, F.J., 1976, Timber-harvesting, mass erosion, and steepland forest geomorphology, *in* Coates, D.R., ed., Geomorphology and Engineering: Stroudsburg, Pennsylvania, Dowden, Hutchinson & Ross, p. 199–221.

Talbot, M.R, Holm, K., and Williams, M.A.J., 1994, Sedimentation in low-gradient desert margin systems: a comparison of the Triassic of northwest Somerset (England) and the late Quaternary of east central Australia, *in* Rosen, M.R., ed., Paleoclimate and Basin Evolution of Playa Systems: Geological Society of America, Special Paper 289, p. 97–117.

Tanaka, J., Yokoi, Y., Kosaki, Y., and Kyuma, K., 1999, Mechanisms and processes of crust formation on artificial aggregates. III Relations between natural rainfall characteristics and degree of crusting: Soil Science and Plant Nutrition, v. 45, p. 537–548.

Tandon, S.K., and Narayan, D., 1981, Calcrete conglomerate, case-hardened conglomerate, and cornstone—a comparative account of pedogenic and nonpedogenic carbonates from the continental Siwalik Group, Punjab, India: Sedimentology, v. 28, p. 353–367.

Tate, T.A., and Retallack, G.J., 1995, Thin sections of paleosols: Journal of Sedimentary Research, v. A65, p. 579–580.

Triplehorn, D.M., Bohor, B.F., and Betterton, W.J., 2002, Chemical disaggregation of kaolinitic claystones (tonsteins and flint clays): Clays and Clay Minerals, v. 50, p. 766–770.

Twitchett, R.J., Looy, C.V., Morante, R., Visscher, H., and Wignall, P.B., 2001, Rapid and synchronous collapse of marine and terrestrial ecosystems during the end-Permian biotic crisis: Geology, v. 29, p. 351–354.

Van Houten, F.B., 1969, Geology of selected areas in New Jersey and eastern Pennsylvania and guidebook of excursions: New Brunswick, New Jersey, U.S.A., Rutgers University Press, p. 314–317.

Visscher, H., Brinkhuis, K., Dilcher, D.L., Elsik, W.C., Eshet, Y., Looy, C., Rampino, M.R., and Traverse, A., 1996, The terminal Paleozoic fungal event: evidence of terrestrial ecosystem destabilization and collapse: U.S. National Academy of Sciences, Proceedings, v. 93, p. 2135–2158.

Walker, G.W., and MacLeod, N.S., 1991, Geologic map of Oregon: Portland, Oregon, U.S.A., Oregon Department of Geology and Mineral Industries, 2 p.

Wang, Z.-Q., 1996, Recovery of vegetation from the terminal Permian mass extinction in north China: Review of Palaeobotany and Palynology, v. 9, p. 121–124.

Ward, P.D., Montgomery, D.R., and Smith, R., 2000, Altered river morphology in South Africa related to the Permian–Triassic extinction: Science, v. 289, p. 1740–1743.

Ward, P.D., Botha, J., Buick, R., De Kock, M.O., Erwin, D.H., Garrison, G., Kirschvink, J., and Smith, R., 2005, Abrupt and gradual extinction among Late Permian land vertebrates in the Karoo Basin, South Africa: Science, v. 307, p. 709–714.

Waterhouse, J.B., 1967, Upper Permian (Tatarian) brachiopods from New Zealand: New Zealand Journal of Geology and Geophysics, v. 10, p. 74–118.

Waterhouse, J.B., 1998, Permian geology of Wairaki Downs, New Zealand, and the realignment of its biozones with the international standard: Royal Society of Victoria, Proceedings, v. 110, p. 235–245.

Wignall, P.B., and Twitchett, R.J., 1999, Unusual intraclastic limestones in Lower Triassic carbonates and their bearing on the aftermath of the end-Permian mass extinction: Sedimentology, v. 46, p. 303–316.

Wignall, P.B., Morante, R., and Newton, R., 1998, The Permo-Triassic transition in Spitsbergen: $\delta^{13}C_{org}$ chemostratigraphy, Fe and S geochemistry, facies, fauna and trace fossils: Geological Magazine, v. 135, p. 47–62.

Witzke, B.J., and Anderson, R.R., 1996, Sedimentary-clast breccias of the Manson impact structure, *in* Koeberl, C., and Anderson, R.R., eds., The Manson Impact Structure, Iowa: Anatomy of an Impact Crater: Geological Society of America, Special Paper, v. 302, p. 115–144.

Wondzell, S.M., and King, J.G., 2003, Post-fire erosional processes in the Pacific Northwest and Rocky Mountain regions: Forest Ecology and Management, v. 178, p. 75–87.

Young, G.M., and Long, D.G.E., 1976, Ice-wedge casts from the Huronian, Ramsay Lake Formation (2300 m.yr.) near Espanola, northern Canada: Palaeogeography, Palaeoclimatology, Palaeoecology, v. 19, p. 191–200.

Zhang, B., and Horn, R., 2001, Mechanisms of aggregate stabilization in Ultisols from subtropical China: Geoderma, v. 99, p. 123–145.

Zhou, Y.-Q., and Chai, C.-F., 1997, The discovery of shocked quartz and stishovite in the Permian/Triassic boundary clay of Huangshi, China: Meteoritics, v. 26, p. 413.

Received 30 March 2004; accepted 25 January 2005.